DEUTSCHES ELEKTRONEN-SYNCHROTRON DESY

DESY 67/34
November 1967

Measurements on Inelastic Electron Proton Scattering

by

F.W. Brasse and J. Engler
Deutsches Elektronen-Synchrotron DESY, Hamburg

E. Ganssauge
Universität Marburg

and

M. Schweizer
II. Physikalisches Institut der Universität Hamburg

2 HAMBURG 52 · NOTKESTIEG 1

DESY-Bericht 67/34 November 1967

Measurements on inelastic Electron Proton Scattering

by

F.W. Brasse, J. Engler, E. Ganßauge, M. Schweizer

Abstract

The cross section for inelastic electron proton scattering has been measured by detecting a) the scattered electron alone and b) by detecting the electron in coincidence with the proton.

Data without coincidence have been taken at scattering angles of 47.5°, 55° and 75° for momentum transfers to the pion nucleon system of 20 and 40 f^{-2} at the first resonance (W = 1236 MeV). One measurement at 32.2° and 40 f^{-2} and one at 47.5° and 60 f^{-2} is also reported here. W has been varied for fixed primary energy from 938 to about 1400 MeV. In addition for $q^2_{1236} = 40\ f^{-2}$, $\vartheta_e = 32.2^{\circ}$ and 47.5° and for $q^2_{1236} = 60\ f^{-2}$ and 47.5° W has been varied up to about 1900 MeV.

At the first resonance the cross sections are compared with results of other laboratories as well as with theoretical predictions based both on symmetry groups and dispersion relations. For the latter case there is quite good agreement with the measurements.

In the region of the second and third classical resonance cross sections do not agree with the threshold behaviour of the resonant parts in this region of momentum transfer. The cross sections, divided by the normalized squared nucleon form factor, increase with $|\vec{q}|^b$, where b increases with W.

In the case of the first resonance at $q^2_{1236} = 20\ f^{-2}$ coincidence measurements between the scattered electron and the proton have been made in order to separate π^o from π^+ - production. The proton has been detected at different CM-angles and at different values of W of the pion nucleon system. Here the measurements differ from the results of the dispersion relation treatment.

1.) Detection of the scattered electron alone

The measurements were made with the two experimental arrangements which had been used for the elastic electron proton scattering[1)-3)], and which are located at two different H_2-targets inside the tunnel of the DESY synchrotron.

One arrangement consists of two single quadrupole spectrometers which can swing around the target. Both spectrometers have scintillation counters, defining 4 momentum channels (slat counters), and a Čerenkov and a shower counter for the identification of the electron. A vertical beam clipper was used inside the synchrotron to cut down the vertical size of the effective target area in order to have sufficient momentum resolution. In contrast to the elastic measurements, the clipper was opened to about one centimeter in order to increase the number of multiple traversals and thereby the effective intensity of the primary electrons. Thus the momentum resolution of the two quadrupole spectrometers was approximately 4.2%.

The other arrangement is a sloped-window-type spectrometer consisting of two quadrupoles and a bending magnet, which again can swing around another internal H_2-target. A set of scintilla-

tion counters in the focal plane defines 7 adjacent momentum channels with a total acceptance of 2.8% and each having a resolution of about 0.8%. Since the resolution of this spectrometer is not influenced by the vertical target size, no beam clipper is necessary and therefore a larger number of multiple traversals through the target can be used than with the quadrupole spectrometers (see also ref. 2). Again a Čerenkov counter and a shower counter are used to identify electrons.

In both arrangements a quantameter monitored the intensity of the primary beam. At each measurement however the absolute calibration was achieved by measuring the elastic scattering both by detecting electrons at the same scattering angle as in the inelastic measurement and by detecting recoil protons at a low momentum transfer (q^2 = 10 resp. 13 f^{-2}). For these reference cross sections form factors were used which were taken from empirical short range fits to the form factors published[1)-5)]. By this method corrections and uncertainties such as bremsstrahlung coming from the target walls, quantameter and integrator calibration and Čerenkov counter efficiency are eliminated.

The contribution to the counting rate coming from the target walls (a cylinder of 11 mm diameter made of 12μ Dupont H film) was measured by replacing the full target by a piece of the foil material presenting the same number of radiation lengths to the primary electrons as the full target.

The data were further corrected for dead time loss, proton loss in the proton reference measurement, and radiation loss at the reference cross sections. The radiation of the electron during the inelastic scattering, and the bremsstrahlung were calculated according to the peaking method[6)]. For the radiative correction (Schwinger effect) a formula of Yennie, Frautschi and Suura[7)] was used. At extremly high values of W the calculation of the radiation during the inelastic scattering may involve a systematic error due to the integration along the whole spectrum, which may not be negligible.

Fig. 1 shows the corrected spectrum of the elastic peak and the first resonance, which was taken with the spectrometer having the better resolution. The dashed line is the sum of the bremsstrahlung and the radiative correction. Just below threshold the calculated bremsstrahlung agrees quite well with the measured cross section.

The cross section for detecting the electron only can be written in the form[8)]

$$\frac{d^2\sigma}{d\Omega dE'} = \Gamma_t \sigma_t + \Gamma_\ell \sigma_\ell = \frac{\alpha}{2\pi^2} \frac{E'}{E} \frac{K}{q^2(1-\varepsilon)} \{\sigma_t + \varepsilon \sigma_\ell\}$$

with the polarization of the virtual photon

$$\varepsilon = \frac{\Gamma_\ell}{\Gamma_t} = (1+2 \frac{|\vec{q}|^2}{q^2} \operatorname{tg}^2 \frac{\vartheta}{2})^{-1}$$

and

$$q^2 = |\vec{q}|^2 - q_o^2 = 4 E E' \sin^2 \vartheta/2$$

being the momentum transfer to the pion nucleon system. E and E' are the energies of the incoming and outgoing electrons. σ_t and σ_ℓ are the cross sections for transverse and longitudinal photons. K is equal to $(W^2 - M^2)/2M$, with W being the mass of the pion nucleon system and M the nucleon mass.

Since

$$|\vec{q}|^2 = (K + \frac{q^2}{2M})^2 + q^2$$

depends only on the mass W for fixed q^2, the value

$$\Sigma_t = \frac{1}{\Gamma_t} \frac{d^2\sigma}{d\Omega dE'}$$

plotted against ε should give a straight line analogous to the Rosenbluth straight line in elastic scattering for a given momentum transfer. The slope of this straight line gives the

longitudinal contribution to the cross section, which is generally expected to be small compared with the transverse part. For $q^2 \to 0$ K becomes the laboratory energy of the real photon and Σ_t approaches the photoproduction cross section.

Figures 2-4 show those spectra which have been extended to higher masses than the first resonance. Σ_t is plotted versus E' and W. The elastic scattering cannot be shown in this representation. The measurements in Fig. 2 and 3 were made with the narrow resolution spectrometer, whereas the spectrum in Fig. 4 was taken with one of the single-quadrupole spectrometers. Three large bumps clearly show up at the position of the first three classical resonances. Whether the second and the third are due to the $D_{13}(1525)$ and F_{15} (1688) respectively or are complicated mixtures of all the resonances known from π-N-scattering cannot be decided presently.

The cross sections at the resonance masses and at some masses between are given in Table 1. The complete data, including the total radiation correction, for all values of W at which measurements have been made, are given in Tables 2-10. The errors in Table 1 contain the statistical errors of the inelastic, the elastic and the background measurements and possible systematical errors for the elastic reference measurements and for the background subtraction. The errors for the inelastic measurement in Tables 2-10 are the statistical ones.

At the first resonance and at W = 1353 MeV we have used the data for a Rosenbluth plot (Figure 5-8). There is an indication of a longitudinal contribution at $q^2 = 20$, but because of the rather small range in ε avaible for these measurements the errors for σ_ℓ are large. The straight lines in Figs. 5 and 6 are theoretical predictions[14] (see below).

For a small longitudinal contribution Σ_t is practically equal to σ_t. If one further assumes that the main contributions to the production come from diagrams, where the virtual photon is

coupled to a nucleon, it is reasonable to divide Σ_t by the square of the magnetic form factor of the proton, normalized to one at $q^2 = 0$. This expression is plotted against $|\vec{q}|^2$ in Figure 9 for W = 1236 MeV in a logarithmic scale in both dimensions. Lynch et al.[9] have separated their data into σ_t and σ_ℓ. They find an increasing longitudinal contribution up to 27% at $q^2 \leq 7.7\ f^{-2}$. Therefore for their data in Figure 9 σ_t is plotted instead of Σ_t.

The data are compared with a model[10], where the nonresonant background is described by the three one-particle exchange diagrams. At the photon vertices, on-shell form factors have been inserted with the following assumptions for the pion and nucleon form factors:

$$F_\pi(q^2) = 1/(1 + q^2/m_\rho^2),$$

$$G_{EN} = 0, \quad G_{EP} = G_{MP}/\mu_P, \quad G_{MN} = G_{MP}\mu_N/\mu_P.$$

G_{MP} has been taken from measurements[1)-5)]. Gauge invariance was restored by the method of Fubini, Nambu and Wataghin[11].

The magnetic dipole contribution in the isospin 3/2-state of these diagrams was subtracted and replaced by the expression

$$M_{1+}^{3/2}(W,q^2) = M_1^{3/2}(W,0) \cdot \frac{|\vec{q}_{CM}|}{|\vec{q}_{CM,o}|} \cdot \left(\frac{E_1+M}{E_{10}+M}\right)^{1/2} \cdot G^*(q^2)$$

where $(E_1, -\vec{q}_{CM})$ is the four momentum of the incoming nucleon in the CM system of the N*, $(E_{10}, -\vec{q}_{CM,o})$ is the same taken for $q^2 = 0$, and M is the nucleon mass. For $M_{1+}^{3/2}(W,0)$ the well-known result of the static theory[12] was inserted:

$$M_{1+}^{3/2}(W,0) = \frac{|\vec{q}_{CM,o}|}{|\vec{k}|} \cdot \frac{\mu_p - \mu_n}{2f} \quad f_{1+}^{3/2}(W)$$

with $\vec{k}$ = outgoing pion momentum in the CM-system of the N*, $f^2 = 0.081$, $f_{1+}^{3/2}(W)$ = (π,N) - scattering amplitude in the N*-channel.

The following choices of $G^*(q^2)$ are compared with the measurements:

1) The $\tilde{U}(12)$ prediction[13],

$$G^*(q^2) = G_{MV}(q^2)/G_{MV}(0),$$

normalized to $G^*(0) = 1$.

2) The prediction from a dispersion theoretic model with inclusion of box diagrams[14]

$$G^*(q^2) = \frac{G_{MV}(q^2)}{G_{MV}(0)} \cdot \frac{0.85}{1+\frac{q^2}{2.9\,GeV^2}} + F_\pi(q^2) \cdot \frac{0.15}{1+\frac{q^2}{0.97\,GeV^2}}$$

3) The results obtained by Zagury[15] from a dispersion theoretic model containing a cut-off, which have been normalized at $q^2 = 0$ to the static theory.

The electric and the longitudinal multipoles E_{1+} and L_{1+} have not been changed with respect to their Born terms contained in the one particle exchange diagrams. The static expression for $M_{1+}^{3/2}$ probably does not give a perfect description of π^0-photoproduction experiments; nevertheless it was used for the normalization as a convenient reference formula.

Fig. 9 contains the results of these predictions for the sum of π^+ and π^0-production, integrated over the total phase space of the proton. The dispersion relation model is clearly in better agreement with the experimental results than the $\tilde{U}(12)$ prediction.

The cross sections for higher masses W, resonant as well as non-resonant, are shown in Figures 10-13. The photoproduction points correspond to total photoabsorption, taken from single and multiple π-production in counter and bubble chamber experiments[16].

Except for the highest values from Cone et al.[17] the data lie on straight lines in the double logarithmic scale.

This means that the cross section shows the behaviour

$$\frac{d^2\sigma}{d\Omega dE'} \approx |\vec{q}|^b \cdot \Gamma_t \cdot G_{MP}^2(q^2);$$

The exponent b is plotted against $K = (W^2 - M^2)/2M$ in Fig. 14. One sees that b increases continuously with increasing W. In the case of the two 1525 and 1688 MeV resonances we have subtracted the nonresonant part as indicated in Figure 2 by the dashed line, which is of course somewhat ambiguous. The corresponding cross sections are also shown in Figures 11 and 13. The resultant exponent b for this cross section is even higher than the one for the total cross section.

The 1525 resonance is known from photoproduction to proceed mainly through an electric dipole transition. This gives a threshold behaviour $\Sigma_t \approx |\vec{q}|^2 G_{MP}^2(q^2)$, which clearly is no longer fulfilled in this region of $|\vec{q}|$. If the resonance would be dominated by the longitudinal transition in electroproduction, the threshold behaviour should be $\frac{1}{\Gamma_\ell}\frac{d^2\sigma}{d\Omega dE'} \approx q^2 G_{MP}^2(q^2)$,[18] which also is not in agreement with the measurements.

The 1688 resonance is known to have mainly an electric quadrupole transition, with a threshold behaviour $|\vec{q}|^2 G_{MP}^2(q^2)$. This again is not valid in this range of momentum transfer.

Therefore one might conclude that the threshold behaviour is no longer valid in this range of momentum transfer or that other nonresonant angular momentum states are involved. It might also mean that diagrams where the virtual photon is coupled to a pion, dominate, and that therefore one should not separate out the nucleon form factor.

2.) Coincidence measurements

In a limited range of the kinematics the two one-quadrupole spectrometers could be used to measure coincidences between the electron and the proton. For this purpose a proton dE/dx counter was installed behind the momentum defining counters in one of the two spectrometers. In addition for discrimination against positive pions the time of flight of the protons was measured with respect to that of the electrons by means of a time to pulse-height converter. This pulse-height and the pulse-height of the dE/dx counter were analyzed two-dimensionally. For the coincidence the full momentum acceptance of 6.7% in both spectrometers was used, whereas for the single arm measurements, taken simultaneously in one of the two spectrometers, also the slat counters were used. The contribution from the target walls to the coincidence rate was measured in the same way as was described for the single arm measurements. It was found to be less than 2%.

The solid angle $d\Omega_{p,CM}$ in the CM system of the pion and nucleon has been calculated by a Monte Carlo program, where the dimensions of the entrance slits and the measured momentum-acceptance distributions (high-energy side of the elastic peak) of the two spectrometers were inserted. Absolute calibration of primary intensity was achieved by referring to elastic single-arm measurements.

The contribution from bremsstrahlung to the coincidence rate (the detected electron and proton belong to the process $e + p \rightarrow e + p + \gamma$) was calculated[19] to be zero except for the peaking directions, where the gamma has the direction of the incoming or outgoing electron. In these cases the contribution to the coincidence rate may be very large and depends very much on the exact acceptances in phase space. This leads to a large error in the calculation; therefore measurements close to the peaking directions have been excluded. The correction for radiation within the inelastic graph, where pion production events not having the correct kinematic values fall into the acceptance of the spectrometers, has been calculated in the same way as

in the single arm measurements. In addition only the acceptance of the proton spectrometer was taken into account. For the Schwinger effect finally Kohaupt[20] had shown in the case of elastic scattering, that there is hardly any difference in the radiation loss between e^- single-arm and coincidence measurements, provided that the acceptance for the proton in angle and momentum is as large as it was in this experiment ($\Delta\theta = 3^\circ$, $\frac{\Delta p}{p} = 6.7\%$). It seems reasonable to extend this to the inelastic scattering.

In Table 11 the results of the coincidence measurements are summarized. $\theta_{p,CM}$ and ϕ are the polar and azimuthal angle of the proton measured in the CM-system of the pion and nucleon with $\vec{q}$ being the polar axis. All measurements are taken for an averaged value of ϕ equal to 0° (in the plane defined by the incoming and outgoing electron). As in the case of the single arm measurements, measurements for different masses W around the first resonance and at $\theta_{p,CM} = 90^\circ$ are compared in Figures 15 a and b with the dispersion theoretic model[14]. Here the agreement is worse. The fact that the discrepancy between the measurements and the calculation depends on the polarization of the photon indicates that the longitudinal contributions are not properly taken into account by the theoretical Ansatz.

We would like to thank Dr. F. Gutbrod for the calculations on the theoretical model and for many stimulating discussions. We appreciate the assistance of Dr. R.D. Kohaupt in calculating the radiation corrections. Mr. J. Gayler did most of the actual calculations of the radiation corrections; we thank him very much for this. Furthermore it is a pleasure to acknowledge the help of Dr. W. Flauger and Mr. W. Albrecht in performing one of the runs.

We are indebted to Professors W. Jentschke and P. Stähelin for their continuous interest and support of this work.

References:

1) H.-J. Behrend, F.W. Brasse, J. Engler, H. Hultschig, S. Galster, G. Hartwig, H. Schopper and E. Ganßauge: Nuov. Cim. 48, 140 (1967)

2) W. Albrecht, H.-J. Behrend, F.W. Brasse, W. Flauger, H.Hultschig and K.G.Steffen:Phys.Rev.Let.17,1192(1966)

3) W. Albrecht, H.-J. Behrend, H. Dorner, W. Flauger and H. Hultschig: Phys. Rev. Let. 18, 1014 (1967)

4) T. Janssens, E.B. Hughes, M.R. Yearian and R. Hofstadter: Phys. Rev. 142, 922 (1966)

5) W. Bartel, B. Dudelzak, H. Krehbiel, J.M. McElroy, U. Meyer-Berkhout, R.J. Morrison, H. Nguyen-Ngoc, W. Schmidt and G. Weber: Phys. Rev. Let. 17, 608 (1966)

6) H. Nguyen-Ngoc and J.P. Perez-y-Jorba: Phys. Rev. 136, B 1036 (1964); see also 8)

7) D.R. Yennie, S.C. Frautschi and H. Suura: Ann.Phys. 13, 379 (1961)

8) L.N. Hand: Phys. Rev. 129, 1834 (1963)

9) H.L. Lynch, J.V. Allaby and D.M. Ritson: HEPL-494 B (1967)

10) The calculations on all three models have been transfered to us by private communication from F. Gutbrod

11) Fubini, Nambu and Wataghin: Phys. Rev. 112, 329 (1958)

12) G.F. Chew, M.L. Goldberger, F. Low and Y. Nambu: Phys. Rev. 106, 1345 (1957)

13) A. Salam, R. Delbourgo and J. Strathdee: Proc.Roy.Soc. (London) A 284, 146 (1965)

14) F. Gutbrod and D. Simon: Nuov.Cim. 51A, 602 (1967)

15) N. Zagury: Phys. Rev. 145, 1112 (1966)

16) Data Compilation by J.T. Beale, S.D. Ecklund, R.L. Walker: Report CTSL-42,CALT-68-108; Aachen-Berlin-Bonn-Hamburg-Heidelberg-München Collaboration ~~DESY 65/11 and~~ DESY 66/32; Cambridge Bubble Chamber Group Phys. Rev. 155, 1477 (1967)

17) A.A. Cone, K.W. Chen, J.R. Dunning, G. Hartwig, N.F.Ramsey, J.K. Walker, R. Wilson: Phys.Rev. 156, 1490 (1967)

18) J.D. Bjorken and J.D. Walecka: Ann.of Phys. 38, 35 (1966)

19) R.D. Kohaupt: Private communication

20) R.D. Kohaupt: Z. f. Phys. 194, 18 (1966)

Table 1: Cross sections from single arm measurements for π-Electroproduction. The measurements at ϑ = 32.2°, 55.0°, 57.0° and 75.0° are made with the single quadrupole spectrometers, the other with the spectrometer having better resolution.

q^2 [f^{-2}]	θ [°]	E [GeV]	E' [GeV]	ε	$\frac{1}{\Gamma_t}\frac{d^2\sigma}{d\Omega dE'}$ [10^{-28} cm^2/ster]
W = 1236 MeV					
19.7	74.9	1.191	0.436	0.326	2.08 ± 6 %
20.0	75.0	1.198	0.438	0.328	2.55 ± 11 %
20.0	55.0	1.408	0.648	0.514	2.68 ± 11 %
19.7	47.4	1.531	0.777	0.599	2.27 ± 5 %
39.6	74.9	1.759	0.592	0.312	0.70 ± 7 %
40.0	57.0	2.016	0.842	0.470	0.83 ± 15 %
39.5	47.4	2.231	1.067	0.580	0.75 ± 6 %
40.0	32.2	2.913	1.738	0.761	0.66 ± 11 %
59.2	47.4	2.835	1.261	0.556	0.32 ± 7 %
W = 1420 MeV					
33.9	47.4	2.231	0.920	0.531	0.43 ± 7 %
36.4	32.2	2.913	1.562	0.722	0.50 ± 11 %
53.2	47.4	2.835	1.129	0.519	0.52 ± 8 %
W = 1525 MeV					
30.6	47.4	2.231	0.826	0.494	0.72 ± 7 %
33.4	32.2	2.913	1.451	0.696	0.69 ± 11 %
49.1	47.4	2.835	1.046	0.492	0.43 ± 8 %
W = 1615 MeV					
27.4	47.4	2.231	0.741	0.458	0.54 ± 7 %
31.0	32.2	2.913	1.348	0.665	0.65 ± 11 %
45.7	47.4	2.835	0.970	0.467	0.29 ± 8 %
W = 1688 MeV					
24.8	47.4	2.231	0.668	0.423	0.77 ± 7 %
29.0	32.2	2.913	1.261	0.637	0.77 ± 11 %
42.5	47.4	2.835	0.904	0.444	0.49 ± 8 %
W = 1820 MeV					
19.6	47.4	2.231	0.529	0.351	0.68 ± 7 %
25.2	32.2	2.913	1.094	0.578	0.63 ± 15 %
36.7	47.4	2.835	0.779	0.396	0.40 ± 8 %

Table 2: Kinematic values and cross sections for the measurement $E = 1.408$ GeV, $\vartheta = 55^\circ$, taken with the single-quadrupole spectrometers.

E' [GeV]	W [GeV]	q^2 [GeV^2]	ε	$\frac{d^2\sigma}{d\Omega dE'}$ $\left[\frac{cm^2}{sterGeV}\right]$	stat. error [%]	$\frac{1}{\Gamma_t}\frac{d^2\sigma}{d\Omega dE'}$ $\left[\frac{cm^2}{ster}\right]$	Rad. correction $\left[\frac{cm^2}{sterGeV}\right]$
0.771	1.073	0.925	0.562	7.60E-33	5.9	1.06E-28	1.37E-33
0.760	1.088	0.913	0.558	8.54E-33	5.7	1.07E-28	1.16E-33
0.751	1.101	0.901	0.555	1.02E-32	5.3	1.17E-28	8.84E-34
0.736	1.121	0.884	0.550	1.05E-32	5.3	1.07E-28	1.11E-33
0.725	1.137	0.870	0.546	1.20E-32	5.0	1.14E-28	1.02E-33
0.704	1.165	0.845	0.538	2.01E-32	4.1	1.68E-28	-2.08E-34
0.697	1.173	0.837	0.535	2.56E-32	3.7	2.05E-28	-1.00E-33
0.683	1.192	0.820	0.529	3.47E-32	3.3	2.59E-28	-1.98E-33
0.671	1.207	0.806	0.524	3.90E-32	3.1	2.76E-28	-1.88E-33
0.653	1.229	0.785	0.517	4.10E-32	3.0	2.70E-28	-1.02E-33
0.645	1.240	0.774	0.513	4.14E-32	3.0	2.63E-28	-4.70E-34
0.635	1.253	0.762	0.508	3.98E-32	3.1	2.44E-28	2.92E-34
0.624	1.266	0.749	0.503	3.81E-32	3.1	2.25E-28	1.21E-33
0.605	1.288	0.727	0.494	3.35E-32	3.3	1.86E-28	2.53E-33
0.598	1.297	0.718	0.491	3.42E-32	3.3	1.86E-28	2.75E-33
0.587	1.309	0.705	0.486	3.52E-32	3.3	1.86E-28	2.88E-33
0.578	1.320	0.694	0.481	3.38E-32	3.3	1.75E-28	3.29E-33
0.540	1.364	0.649	0.461	2.01E-32	4.1	9.50E-29	6.21E-33
0.533	1.372	0.640	0.457	2.11E-32	4.0	9.83E-29	6.23E-33
0.524	1.382	0.629	0.451	2.27E-32	4.0	1.03E-28	5.87E-33
0.515	1.392	0.619	0.446	2.57E-32	3.8	1.16E-28	5.66E-33
0.477	1.433	0.573	0.424	2.30E-32	4.1	9.70E-29	7.03E-33

Table 3: Kinematic values and cross sections for the measurement E = 1.198 GeV, $\vartheta = 75^{\circ}$, taken with the single-quadrupole spectrometers.

E' [GeV]	W [GeV]	q^2 [GeV^2]	ε	$\frac{d^2\sigma}{d\Omega dE'}$ $\left[\frac{cm^2}{sterGeV}\right]$	stat. error [%]	$\frac{1}{\Gamma_t}\frac{d^2\sigma}{d\Omega dE'}$ $\left[\frac{cm^2}{ster}\right]$	Rad. correction $\left[\frac{cm^2}{sterGeV}\right]$
0.541	1.073	0.961	0.370	3.21E-33	18.9	8.06E-29	9.91E-34
0.534	1.085	0.948	0.367	3.40E-33	18.9	7.81E-29	8.59E-34
0.525	1.101	0.932	0.364	4.53E-33	17.1	9.38E-29	7.32E-34
0.516	1.115	0.917	0.360	4.87E-33	16.7	9.28E-29	7.92E-34
0.511	1.123	0.907	0.358	4.46E-33	17.4	8.10E-29	7.80E-34
0.504	1.135	0.894	0.356	7.71E-33	13.9	1.31E-28	6.71E-34
0.495	1.149	0.879	0.352	6.90E-33	14.9	1.10E-28	4.74E-34
0.491	1.155	0.872	0.351	1.00E-32	12.6	1.55E-28	3.85E-34
0.484	1.167	0.859	0.348	1.05E-32	12.5	1.53E-28	2.84E-34
0.475	1.180	0.844	0.344	1.29E-32	11.5	1.79E-28	-1.39E-34
0.470	1.188	0.835	0.342	1.79E-32	10.0	2.39E-28	-5.98E-34
0.466	1.194	0.827	0.340	2.20E-32	9.1	2.87E-28	-8.91E-34
0.457	1.209	0.811	0.336	2.27E-32	9.0	2.81E-28	-8.60E-34
0.450	1.218	0.800	0.333	2.32E-32	8.9	2.76E-28	-4.29E-34
0.444	1.227	0.788	0.330	2.18E-32	9.1	2.52E-28	9.88E-35
0.437	1.238	0.775	0.327	2.10E-32	9.3	2.33E-28	4.12E-34
0.429	1.249	0.762	0.324	2.34E-32	8.9	2.52E-28	5.81E-34
0.423	1.258	0.751	0.321	2.26E-32	9.1	2.36E-28	7.72E-34
0.416	1.269	0.738	0.317	2.38E-32	8.8	2.40E-28	1.22E-33
0.407	1.281	0.723	0.313	1.97E-32	9.6	1.93E-28	1.99E-33
0.402	1.288	0.714	0.310	1.67E-32	10.3	1.59E-28	2.30E-33
0.396	1.297	0.703	0.307	2.10E-32	9.4	1.96E-28	2.21E-33
0.390	1.306	0.692	0.304	2.41E-32	8.9	2.20E-28	2.13E-33
0.354	1.355	0.628	0.285	1.51E-32	10.8	1.22E-28	4.41E-33
0.348	1.363	0.617	0.281	1.34E-32	11.4	1.06E-28	4.57E-33
0.341	1.372	0.606	0.278	1.96E-32	10.1	1.52E-28	3.76E-33
0.336	1.379	0.597	0.275	1.81E-32	10.5	1.39E-28	3.85E-33
0.306	1.418	0.543	0.256	1.99E-32	10.5	1.41E-28	4.00E-33
0.302	1.424	0.535	0.254	2.61E-32	9.4	1.83E-28	4.06E-33
0.296	1.430	0.526	0.250	2.64E-32	9.4	1.84E-28	4.26E-33
0.291	1.437	0.517	0.247	3.01E-32	9.0	2.06E-28	4.26E-33

Table 4: Kinematic values and cross sections for the measurement $E = 2.913$ GeV, $\vartheta = 32.2^{\circ}$, taken with the single-quadrupole spectrometers.

E' [GeV]	W [GeV]	q^2 [GeV^2]	ε	$\frac{d^2\sigma}{d\Omega dE'}$ $\left[\frac{cm^2}{sterGeV}\right]$	stat. error [%]	$\frac{1}{\Gamma_t}\frac{d^2\sigma}{d\Omega dE'}$ $\left[\frac{cm^2}{ster}\right]$	Rad. correction $\left[\frac{cm^2}{sterGeV}\right]$
1.870	1.077	1.676	0.785	5.16E-33	13.9	5.25E-29	1.40E-34
1.846	1.109	1.654	0.780	4.96E-33	14.4	4.13E-29	-5.09E-36
1.821	1.140	1.631	0.776	6.62E-33	12.7	4.69E-29	-1.24E-34
1.793	1.172	1.607	0.771	1.02E-32	10.5	6.26E-29	-6.47E-34
1.768	1.202	1.584	0.767	1.13E-32	10.1	6.22E-29	-7.76E-34
1.743	1.230	1.562	0.762	1.32E-32	9.3	6.60E-29	-6.68E-34
1.724	1.252	1.544	0.759	1.26E-32	9.6	5.87E-29	-6.40E-34
1.719	1.258	1.540	0.757	1.36E-32	9.2	6.24E-29	-6.19E-34
1.694	1.285	1.517	0.752	1.36E-32	9.2	5.79E-29	-4.17E-34
1.669	1.311	1.495	0.747	1.27E-32	9.5	5.08E-29	-1.54E-34
1.644	1.337	1.473	0.741	1.33E-32	9.3	5.01E-29	5.51E-35
1.619	1.363	1.450	0.736	1.39E-32	9.2	4.99E-29	6.87E-35
1.594	1.388	1.428	0.730	1.44E-32	9.1	4.92E-29	6.22E-35
1.569	1.413	1.406	0.724	1.58E-32	8.7	5.17E-29	1.25E-34
1.542	1.439	1.381	0.719	1.62E-32	8.7	5.08E-29	1.50E-34
1.517	1.463	1.359	0.711	1.78E-32	8.4	5.40E-29	-8.89E-35
1.492	1.487	1.337	0.705	2.16E-32	7.8	6.34E-29	-4.84E-34
1.467	1.510	1.314	0.699	2.47E-32	7.4	7.06E-29	-6.79E-34
1.442	1.532	1.292	0.692	2.63E-32	7.1	7.32E-29	-3.91E-34
1.417	1.555	1.270	0.685	2.43E-32	7.4	6.59E-29	2.11E-34
1.392	1.577	1.247	0.678	2.46E-32	7.4	6.54E-29	7.39E-34
1.367	1.599	1.225	0.670	2.49E-32	7.4	6.48E-29	9.18E-34
1.345	1.618	1.205	0.664	2.52E-32	7.4	6.46E-29	8.75E-34
1.328	1.633	1.189	0.658	2.62E-32	7.3	6.63E-29	1.10E-33
1.308	1.650	1.172	0.652	2.67E-32	7.2	6.69E-29	1.70E-33
1.303	1.654	1.167	0.651	2.28E-32	7.7	5.69E-29	1.78E-33
1.283	1.670	1.149	0.644	2.98E-32	6.9	7.34E-29	1.31E-33
1.278	1.674	1.145	0.643	2.77E-32	7.2	6.81E-29	1.25E-33
1.258	1.691	1.127	0.636	3.07E-32	6.9	7.47E-29	1.60E-33
1.250	1.697	1.120	0.634	2.82E-32	7.1	6.85E-29	1.81E-33
1.240	1.705	1.111	0.631	2.87E-32	7.1	6.93E-29	1.58E-33
1.233	1.711	1.105	0.628	3.35E-32	6.7	8.06E-29	1.30E-33
1.225	1.717	1.098	0.625	3.23E-32	6.8	7.74E-29	1.18E-33
1.220	1.721	1.093	0.624	3.43E-32	6.6	8.20E-29	1.34E-33
1.208	1.731	1.082	0.620	2.90E-32	7.1	6.91E-29	2.23E-33
1.200	1.737	1.076	0.617	2.88E-32	7.1	6.83E-29	2.68E-33
1.183	1.751	1.060	0.611	3.10E-32	6.9	7.30E-29	2.89E-33
1.176	1.757	1.053	0.608	2.77E-32	7.3	6.52E-29	3.07E-33
1.158	1.771	1.038	0.602	2.95E-32	7.1	6.90E-29	3.57E-33
1.148	1.778	1.029	0.598	2.51E-32	7.6	5.86E-29	3.74E-33
1.133	1.790	1.015	0.593	3.16E-32	6.9	7.32E-29	3.42E-33
1.123	1.798	1.006	0.589	2.89E-32	7.3	6.67E-29	3.39E-33
1.106	1.811	0.991	0.583	3.02E-32	7.1	6.96E-29	3.89E-33
1.098	1.817	0.984	0.580	2.78E-32	7.4	6.39E-29	4.30E-33
1.083	1.828	0.971	0.574	2.70E-32	7.4	6.19E-29	4.80E-33
1.073	1.836	0.962	0.571	2.58E-32	7.6	5.89E-29	4.94E-33
1.059	1.847	0.948	0.565	2.97E-32	7.2	6.76E-29	4.73E-33

Table 4 continued:

E' [GeV]	W [GeV]	q^2 [GeV^2]	ε	$\frac{d^2\sigma}{d\Omega dE'}$ $\left[\frac{cm^2}{sterGeV}\right]$	stat. error [%]	$\frac{1}{\Gamma_t}$	$\frac{d^2\sigma}{d\Omega dE'}$ $\left[\frac{cm^2}{ster}\right]$	Rad. correction $\left[\frac{cm^2}{sterGeV}\right]$
1.049	1.855	0.939	0.561	2.77E-32	7.5		6.29E-29	4.88E-33
1.034	1.866	0.926	0.555	2.85E-32	7.4		6.45E-29	5.29E-33
1.024	1.873	0.917	0.551	2.51E-32	7.8		5.68E-29	5.46E-33
1.009	1.884	0.904	0.545	3.21E-32	7.1		7.25E-29	5.32E-33
0.999	1.891	0.895	0.541	2.85E-32	7.5		6.43E-29	5.28E-33
0.984	1.902	0.881	0.535	3.20E-32	7.2		7.21E-29	4.98E-33
0.974	1.910	0.873	0.531	3.54E-32	7.0		7.96E-29	4.72E-33
0.959	1.920	0.859	0.524	3.99E-32	6.7		8.94E-29	4.88E-33
0.946	1.929	0.848	0.519	3.32E-32	7.2		7.43E-29	5.52E-33
0.934	1.938	0.837	0.514	3.48E-32	7.1		7.79E-29	6.01E-33
0.922	1.947	0.826	0.508	3.61E-32	7.0		8.07E-29	6.14E-33
0.909	1.956	0.814	0.503	3.93E-32	6.8		8.79E-29	6.38E-33
0.897	1.965	0.803	0.498	3.17E-32	7.4		7.08E-29	6.81E-33
0.884	1.974	0.792	0.492	3.99E-32	6.8		8.91E-29	7.11E-33
0.872	1.982	0.781	0.487	3.46E-32	7.2		7.73E-29	7.36E-33
0.859	1.991	0.770	0.481	3.93E-32	6.9		8.76E-29	7.73E-33
0.847	2.000	0.759	0.475	3.34E-32	7.4		7.43E-29	8.07E-33
0.834	2.008	0.748	0.470	4.00E-32	6.9		8.92E-29	8.41E-33
0.822	2.017	0.736	0.464	3.49E-32	7.3		7.78E-29	9.14E-33
0.809	2.025	0.725	0.458	3.43E-32	7.3		7.64E-29	9.98E-33
0.797	2.034	0.714	0.452	2.94E-32	7.8		6.55E-29	1.01E-32
0.785	2.042	0.703	0.446	3.77E-32	7.2		8.41E-29	9.64E-33
0.772	2.051	0.692	0.440	3.60E-32	7.3		8.02E-29	1.04E-32
0.760	2.059	0.681	0.434	3.19E-32	7.6		7.11E-29	1.18E-32

Table 5: Kinematic values and cross sections for the measurement $E = 2.016$ GeV, $\vartheta = 57^\circ$, taken with the single-quadrupole spectrometers.

E' [GeV]	W [GeV]	q^2 [GeV^2]	ε	$\frac{d^2\sigma}{d\Omega dE'}$ $\left[\frac{cm^2}{sterGeV}\right]$	stat. error [%]	$\frac{1}{\Gamma_t}\frac{d^2\sigma}{d\Omega dE'}$ $\left[\frac{cm^2}{ster}\right]$	Rad. correction $\left[\frac{cm^2}{sterGeV}\right]$
0.948	1.070	1.740	0.506	1.53E-33	13.9	5.36E-29	5.17E-35
0.937	1.088	1.720	0.503	1.69E-33	13.4	5.19E-29	3.29E-35
0.927	1.106	1.701	0.500	1.12E-33	16.4	3.08E-29	2.83E-35
0.916	1.123	1.682	0.497	1.84E-33	12.7	4.57E-29	1.07E-34
0.906	1.140	1.663	0.493	2.02E-33	12.5	4.56E-29	2.22E-35
0.895	1.157	1.644	0.490	2.69E-33	11.2	5.61E-29	-1.15E-34
0.874	1.191	1.605	0.484	4.92E-33	8.5	8.89E-29	-3.39E-34
0.864	1.207	1.586	0.480	4.92E-33	8.5	8.35E-29	-3.17E-34
0.853	1.223	1.567	0.477	5.08E-33	8.4	8.13E-29	-2.51E-34
0.843	1.239	1.547	0.473	5.90E-33	7.7	8.94E-29	-1.56E-34
0.832	1.254	1.528	0.470	4.81E-33	8.5	6.92E-29	-2.94E-35
0.822	1.270	1.509	0.466	5.06E-33	8.2	6.94E-29	9.88E-35
0.812	1.285	1.490	0.462	5.01E-33	8.2	6.57E-29	2.11E-34
0.801	1.300	1.471	0.458	4.19E-33	8.9	5.26E-29	3.13E-34
0.791	1.315	1.451	0.455	4.55E-33	8.6	5.50E-29	3.72E-34
0.780	1.329	1.432	0.451	4.36E-33	8.8	5.07E-29	3.77E-34
0.770	1.344	1.413	0.447	4.88E-33	8.5	5.47E-29	3.70E-34
0.759	1.358	1.394	0.443	5.05E-33	8.4	5.48E-29	3.78E-34
0.749	1.373	1.374	0.439	4.93E-33	8.5	5.18E-29	3.81E-34
0.738	1.387	1.355	0.435	5.95E-33	7.9	6.06E-29	3.82E-34
0.728	1.401	1.336	0.431	5.68E-33	8.1	5.61E-29	4.26E-34
0.717	1.414	1.317	0.427	5.82E-33	8.0	5.60E-29	5.28E-34
0.707	1.428	1.298	0.422	5.76E-33	8.0	5.39E-29	6.47E-34
0.696	1.442	1.278	0.418	5.78E-33	8.0	5.28E-29	6.80E-34
0.686	1.455	1.259	0.414	7.00E-33	7.5	6.23E-29	4.89E-34

Table 6: Kinematic values and cross sections for the measurement $E = 1.531$ GeV, $\vartheta = 47.37^{\circ}$, taken with the three-magnet spectrometer. Cross sections are averaged over three adjacent momentum channels.

E' [GeV]	W [GeV]	q^2 [GeV^2]	ε	$\frac{d^2\sigma}{d\Omega dE'}$ $\left[\frac{cm^2}{sterGeV}\right]$	stat. error [%]	$\frac{1}{\Gamma_t}\frac{d^2\sigma}{d\Omega dE'}$ $\left[\frac{cm^2}{ster}\right]$	Rad. correction $\left[\frac{cm^2}{sterGeV}\right]$
0.925	1.050	0.914	0.650	3.40E-34	11.1	4.09E-30	5.10E-33
0.913	1.067	0.902	0.646	1.40E-34	12.1	1.48E-30	4.54E-33
0.902	1.081	0.891	0.643	-3.38E-35	13.2	-3.20E-31	4.00E-33
0.890	1.097	0.879	0.639	2.00E-33	11.3	1.71E-29	3.42E-33
0.879	1.111	0.869	0.636	4.34E-33	9.8	3.43E-29	3.05E-33
0.868	1.126	0.858	0.632	4.52E-33	10.0	3.30E-29	2.61E-33
0.857	1.139	0.847	0.628	7.26E-33	8.8	4.96E-29	2.13E-33
0.846	1.153	0.836	0.625	1.09E-32	7.7	7.01E-29	1.49E-33
0.835	1.166	0.825	0.621	1.63E-32	6.6	9.87E-29	5.73E-34
0.825	1.179	0.815	0.617	2.17E-32	6.0	1.25E-28	-5.47E-34
0.814	1.192	0.805	0.613	3.01E-32	5.2	1.66E-28	-1.96E-33
0.804	1.204	0.795	0.610	4.04E-32	4.5	2.13E-28	-3.05E-33
0.794	1.216	0.785	0.606	4.78E-32	4.2	2.42E-28	-3.24E-33
0.784	1.228	0.775	0.602	4.64E-32	4.3	2.26E-28	-2.88E-33
0.774	1.239	0.765	0.598	4.82E-32	4.2	2.27E-28	-1.82E-33
0.764	1.250	0.755	0.594	4.50E-32	4.3	2.06E-28	-3.51E-34
0.755	1.261	0.746	0.590	4.21E-32	4.4	1.87E-28	1.17E-33
0.745	1.272	0.736	0.586	3.23E-32	4.9	1.39E-28	2.59E-33
0.736	1.282	0.727	0.582	3.06E-32	5.0	1.29E-28	3.44E-33
0.726	1.293	0.718	0.577	2.89E-32	5.1	1.18E-28	3.73E-33
0.717	1.303	0.709	0.573	3.03E-32	5.0	1.21E-28	3.86E-33
0.708	1.313	0.700	0.569	2.61E-32	5.4	1.02E-28	4.15E-33
0.699	1.323	0.691	0.565	2.61E-32	5.4	1.00E-28	4.51E-33
0.691	1.332	0.683	0.561	2.39E-32	5.6	9.00E-29	4.66E-33
0.682	1.342	0.674	0.557	2.43E-32	5.6	8.98E-29	4.72E-33
0.673	1.351	0.665	0.552	2.64E-32	5.4	9.61E-29	4.80E-33
0.665	1.360	0.657	0.548	2.35E-32	5.7	8.43E-29	5.00E-33
0.656	1.368	0.649	0.544	2.14E-32	6.0	7.56E-29	5.17E-33
0.648	1.377	0.640	0.540	2.50E-32	5.6	8.70E-29	5.33E-33
0.640	1.386	0.632	0.535	2.41E-32	5.7	8.27E-29	5.52E-33
0.632	1.394	0.625	0.531	2.08E-32	6.1	7.07E-29	5.63E-33
0.624	1.402	0.616	0.527	2.26E-32	6.0	7.56E-29	5.51E-33
0.616	1.410	0.609	0.523	2.73E-32	5.6	9.03E-29	5.20E-33
0.608	1.418	0.601	0.518	2.84E-32	5.5	9.29E-29	4.90E-33
0.601	1.426	0.593	0.514	2.87E-32	5.6	9.31E-29	4.83E-33
0.593	1.433	0.586	0.510	2.96E-32	5.5	9.49E-29	5.14E-33
0.585	1.441	0.578	0.505	3.28E-32	5.2	1.04E-28	5.82E-33
0.578	1.448	0.571	0.501	2.68E-32	5.7	8.43E-29	6.42E-33
0.571	1.456	0.564	0.496	2.79E-32	5.6	8.72E-29	6.34E-33
0.564	1.462	0.557	0.492	3.22E-32	5.4	9.99E-29	5.57E-33

Table 7: Kinematic values and cross sections for the measurement E = 1.191 GeV, $\vartheta = 74.91^{\circ}$, taken with the three-magnet spectrometer. Cross sections are averaged over three adjacent momentum channels.

E' [GeV]	W [GeV]	q^2 [GeV^2]	ε	$\frac{d^2\sigma}{d\Omega dE'}$ $[\frac{cm^2}{sterGeV}]$	stat. error [%]	$\frac{1}{\Gamma_t}\frac{d^2\sigma}{d\Omega dE'}$ $[\frac{cm^2}{ster}]$	Rad. correction $[\frac{cm^2}{sterGeV}]$
0.553	1.050	0.975	0.376	-5.02E-34	15.0	-1.51E-29	1.91E-33
0.546	1.062	0.962	0.373	-2.77E-34	14.5	-7.46E-30	1.79E-33
0.540	1.073	0.951	0.371	-3.73E-34	16.0	-9.21E-30	1.64E-33
0.532	1.085	0.938	0.368	4.17E-34	13.3	9.42E-30	1.44E-33
0.526	1.096	0.927	0.366	1.08E-33	11.8	2.27E-29	1.29E-33
0.519	1.107	0.915	0.363	1.61E-33	11.0	3.16E-29	1.15E-33
0.513	1.118	0.903	0.361	2.16E-33	10.3	3.98E-29	1.02E-33
0.506	1.128	0.892	0.358	2.98E-33	9.4	5.19E-29	8.97E-34
0.500	1.138	0.881	0.356	4.77E-33	7.9	7.87E-29	7.77E-34
0.494	1.148	0.870	0.354	4.03E-33	8.7	6.34E-29	6.58E-34
0.487	1.159	0.858	0.351	7.28E-33	6.8	1.09E-28	5.12E-34
0.481	1.168	0.848	0.348	7.04E-33	7.0	1.01E-28	3.19E-34
0.475	1.178	0.837	0.346	9.87E-33	6.1	1.36E-28	1.05E-34
0.469	1.187	0.826	0.343	1.22E-32	5.6	1.61E-28	-1.56E-34
0.463	1.196	0.816	0.341	1.25E-32	5.6	1.60E-28	-3.51E-34
0.457	1.205	0.806	0.338	1.75E-32	4.7	2.16E-28	-4.65E-34
0.452	1.213	0.796	0.336	1.61E-32	5.0	1.93E-28	-4.81E-34
0.446	1.222	0.785	0.333	1.86E-32	4.6	2.15E-28	-3.80E-34
0.440	1.230	0.776	0.330	1.91E-32	4.6	2.16E-28	-1.74E-34
0.435	1.238	0.766	0.328	1.98E-32	4.5	2.17E-28	2.84E-34
0.429	1.246	0.756	0.325	1.55E-32	5.0	1.65E-28	8.06E-34
0.424	1.254	0.747	0.323	1.65E-32	4.8	1.71E-28	1.29E-33
0.418	1.262	0.737	0.320	1.38E-32	5.2	1.40E-28	1.69E-33
0.413	1.269	0.728	0.318	1.32E-32	5.3	1.31E-28	1.96E-33
0.408	1.277	0.718	0.315	1.23E-32	5.4	1.20E-28	2.22E-33
0.403	1.284	0.710	0.312	1.03E-32	5.8	9.84E-29	2.32E-33
0.398	1.292	0.701	0.310	1.19E-32	5.6	1.11E-28	2.34E-33
0.393	1.299	0.692	0.307	1.18E-32	5.6	1.08E-28	2.29E-33
0.388	1.305	0.683	0.305	1.08E-32	5.9	9.72E-29	2.29E-33
0.383	1.312	0.674	0.302	1.25E-32	5.5	1.10E-28	2.42E-33
0.378	1.319	0.666	0.300	1.13E-32	5.7	9.84E-29	2.65E-33
0.373	1.326	0.657	0.297	9.08E-33	6.2	7.75E-29	2.96E-33
0.369	1.332	0.649	0.294	8.97E-33	6.3	7.54E-29	3.12E-33
0.364	1.338	0.641	0.292	9.68E-33	6.1	8.01E-29	3.17E-33
0.359	1.345	0.633	0.289	8.68E-33	6.4	7.08E-29	3.10E-33
0.355	1.351	0.625	0.287	1.01E-32	6.1	8.12E-29	2.97E-33
0.350	1.357	0.617	0.284	1.13E-32	5.9	8.96E-29	2.79E-33
0.346	1.362	0.610	0.282	1.20E-32	5.8	9.40E-29	2.76E-33

Table 8a: Kinematic values and cross sections for the meausrement E = 2.231 GeV, $\vartheta = 47.37^{\circ}$, taken with the three-magnet spectrometer. Cross sections are averaged over two adjacent momentum channels.

E' [GeV]	W [GeV]	q^2 [GeV^2]	ε	$\frac{d^2\sigma}{d\Omega dE'}$ $\left[\frac{cm^2}{sterGeV}\right]$	stat. error [%]	$\frac{1}{\Gamma_t}\frac{d^2\sigma}{d\Omega dE'}$ $\left[\frac{cm^2}{ster}\right]$	Rad. correction $\left[\frac{cm^2}{sterGeV}\right]$
1.195	1.050	1.721	0.616	2.76E-34	13.1	7.79E-30	6.51E-34
1.185	1.066	1.706	0.613	1.01E-34	15.4	2.49E-30	5.74E-34
1.176	1.081	1.693	0.610	3.39E-34	13.8	7.48E-30	5.08E-34
1.166	1.095	1.679	0.608	6.14E-34	12.6	1.23E-29	4.16E-34
1.155	1.112	1.663	0.605	7.76E-34	12.2	1.40E-29	3.39E-34
1.146	1.125	1.650	0.603	1.32E-33	10.3	2.21E-29	2.47E-34
1.137	1.139	1.636	0.600	1.53E-33	9.9	2.39E-29	1.83E-34
1.127	1.153	1.622	0.597	2.09E-33	8.7	3.05E-29	1.38E-34
1.117	1.167	1.608	0.595	2.27E-33	8.5	3.11E-29	7.13E-35
1.108	1.180	1.595	0.592	2.88E-33	7.8	3.73E-29	-7.82E-35
1.099	1.193	1.582	0.589	3.79E-33	7.1	4.68E-29	-3.27E-34
1.089	1.207	1.567	0.586	6.15E-33	5.6	7.20E-29	-6.02E-34
1.080	1.219	1.555	0.584	6.83E-33	5.4	7.66E-29	-7.15E-34
1.071	1.231	1.542	0.581	7.19E-33	5.2	7.74E-29	-6.33E-34
1.062	1.243	1.529	0.578	6.88E-33	5.3	7.11E-29	-4.25E-34
1.053	1.255	1.516	0.576	6.35E-33	5.4	6.32E-29	-2.03E-34
1.044	1.266	1.503	0.573	6.36E-33	5.4	6.12E-29	-4.23E-35
1.036	1.278	1.491	0.570	5.53E-33	5.7	5.15E-29	6.76E-35
1.026	1.290	1.477	0.567	5.65E-33	5.7	5.09E-29	1.46E-34
1.018	1.301	1.465	0.565	5.78E-33	5.6	5.06E-29	1.85E-34
1.010	1.311	1.454	0.562	5.35E-33	5.8	4.56E-29	2.51E-34
1.001	1.322	1.441	0.559	5.42E-33	5.8	4.49E-29	3.41E-34
0.992	1.333	1.428	0.556	4.77E-33	6.1	3.85E-29	4.08E-34
0.984	1.343	1.417	0.553	5.13E-33	5.9	4.05E-29	4.35E-34
0.976	1.353	1.405	0.551	5.02E-33	6.0	3.87E-29	4.40E-34
0.967	1.364	1.392	0.548	5.11E-33	6.0	3.85E-29	4.29E-34
0.959	1.373	1.381	0.545	5.34E-33	5.9	3.94E-29	4.10E-34
0.951	1.383	1.370	0.542	5.56E-33	5.8	4.03E-29	4.12E-34
0.943	1.392	1.358	0.539	5.82E-33	5.7	4.13E-29	4.27E-34
0.935	1.402	1.346	0.536	5.58E-33	5.8	3.88E-29	4.19E-34
0.927	1.411	1.335	0.533	6.14E-33	5.6	4.20E-29	3.88E-34
0.920	1.420	1.324	0.531	6.39E-33	5.5	4.30E-29	3.82E-34
0.911	1.430	1.312	0.528	7.20E-33	5.2	4.76E-29	4.45E-34
0.904	1.438	1.302	0.525	5.96E-33	5.7	3.88E-29	5.02E-34
0.897	1.447	1.291	0.522	6.42E-33	5.5	4.13E-29	4.92E-34
0.889	1.456	1.280	0.519	7.70E-33	5.2	4.87E-29	3.81E-34
0.881	1.464	1.269	0.516	8.29E-33	5.0	5.17E-29	2.35E-34
0.874	1.472	1.258	0.513	9.07E-33	4.9	5.59E-29	1.26E-34
0.867	1.480	1.248	0.511	9.51E-33	4.8	5.79E-29	3.66E-35
0.859	1.489	1.237	0.507	1.17E-32	4.4	7.04E-29	-7.40E-35
0.852	1.497	1.227	0.505	1.09E-32	4.6	6.49E-29	-1.73E-34
0.845	1.505	1.217	0.502	1.34E-32	4.1	7.85E-29	-2.23E-34
0.838	1.513	1.206	0.499	1.32E-32	4.2	7.64E-29	-1.63E-34
0.830	1.521	1.196	0.496	1.31E-32	4.2	7.51E-29	5.23E-35
0.824	1.528	1.186	0.493	1.28E-32	4.2	7.25E-29	3.37E-34
0.817	1.535	1.176	0.491	1.16E-32	4.4	6.52E-29	5.88E-34
0.809	1.543	1.165	0.487	1.11E-32	4.5	6.20E-29	7.26E-34
0.803	1.550	1.156	0.485	1.21E-32	4.3	6.68E-29	7.22E-34
0.796	1.557	1.147	0.482	1.26E-32	4.2	6.88E-29	7.55E-34
0.789	1.565	1.137	0.479	1.09E-32	4.5	5.92E-29	9.10E-34

Table 8b: Kinematic values and cross sections for the measurement E = 2.231 GeV, $\vartheta = 47.37^{\circ}$, taken with the three-magnet spectrometer. Cross sections are averaged over four adjacent momentum channels.

E' [GeV]	W [GeV]	q^2 [GeV^2]	ε	$\frac{d^2\sigma}{d\Omega dE'}$ $\left[\frac{cm^2}{sterGeV}\right]$	stat. error [%]	$\frac{1}{\Gamma_t}\frac{d^2\sigma}{d\Omega dE'}$ $\left[\frac{cm^2}{ster}\right]$	Rad. correction $\left[\frac{cm^2}{sterGeV}\right]$
1.190	1.058	1.714	0.614	2.17E-34	10.0	5.71E-30	5.84E-34
1.171	1.088	1.686	0.609	4.93E-34	9.3	1.03E-29	4.45E-34
1.150	1.119	1.656	0.604	1.05E-33	7.9	1.84E-29	2.86E-34
1.132	1.146	1.629	0.599	1.85E-33	6.5	2.80E-29	1.18E-34
1.112	1.174	1.602	0.593	2.75E-33	5.8	3.66E-29	-1.78E-34
1.094	1.200	1.575	0.588	4.92E-33	4.4	5.91E-29	-4.13E-34
1.076	1.225	1.549	0.583	6.90E-33	3.7	7.47E-29	-4.67E-34
1.057	1.249	1.522	0.577	6.60E-33	3.8	6.69E-29	-3.02E-34
1.040	1.272	1.497	0.572	6.00E-33	3.9	5.68E-29	-4.42E-35
1.022	1.295	1.471	0.566	5.67E-33	4.0	5.03E-29	2.12E-34
1.005	1.317	1.447	0.560	5.33E-33	4.1	4.48E-29	3.52E-34
0.988	1.338	1.423	0.555	4.93E-33	4.2	3.94E-29	4.38E-34
0.971	1.358	1.399	0.549	5.04E-33	4.2	3.84E-29	4.55E-34
0.955	1.378	1.375	0.543	5.41E-33	4.1	3.96E-29	4.48E-34
0.939	1.397	1.352	0.538	5.68E-33	4.1	3.99E-29	4.45E-34
0.924	1.415	1.330	0.532	6.19E-33	3.9	4.21E-29	4.56E-34
0.908	1.434	1.307	0.526	6.61E-33	3.9	4.34E-29	4.45E-34
0.893	1.451	1.285	0.521	7.15E-33	3.8	4.56E-29	3.44E-34
0.878	1.468	1.264	0.515	8.71E-33	3.5	5.40E-29	1.53E-34
0.863	1.485	1.242	0.509	1.06E-32	3.2	6.43E-29	-2.77E-35
0.849	1.501	1.222	0.503	1.20E-32	3.1	7.10E-29	-6.05E-35
0.834	1.517	1.201	0.497	1.30E-32	3.0	7.48E-29	1.10E-34
0.820	1.532	1.181	0.492	1.22E-32	3.0	6.92E-29	3.94E-34
0.806	1.547	1.161	0.486	1.16E-32	3.1	6.43E-29	7.35E-34
0.793	1.561	1.142	0.480	1.16E-32	3.1	6.30E-29	1.01E-33
0.779	1.575	1.122	0.475	1.10E-32	3.2	5.88E-29	1.28E-33
0.766	1.589	1.104	0.469	1.01E-32	3.3	5.31E-29	1.46E-33
0.754	1.602	1.085	0.463	9.78E-33	3.3	5.07E-29	1.56E-33
0.741	1.615	1.067	0.457	1.12E-32	3.2	5.74E-29	1.58E-33
0.729	1.628	1.049	0.452	1.12E-32	3.2	5.65E-29	1.55E-33
0.716	1.641	1.031	0.446	1.11E-32	3.2	5.56E-29	1.51E-33
0.704	1.653	1.014	0.441	1.43E-32	2.9	7.03E-29	1.46E-33
0.692	1.664	0.997	0.435	1.36E-32	3.0	6.60E-29	1.45E-33
0.681	1.676	0.980	0.430	1.54E-32	2.9	7.44E-29	1.49E-33
0.669	1.687	0.964	0.424	1.54E-32	2.9	7.37E-29	1.62E-33
0.658	1.698	0.947	0.418	1.69E-32	2.8	8.00E-29	1.83E-33
0.647	1.709	0.932	0.413	1.54E-32	2.9	7.22E-29	2.06E-33
0.636	1.720	0.916	0.408	1.67E-32	2.8	7.75E-29	2.31E-33
0.626	1.730	0.901	0.402	1.54E-32	2.9	7.13E-29	2.51E-33
0.615	1.740	0.885	0.397	1.68E-32	2.8	7.68E-29	2.79E-33
0.605	1.750	0.871	0.392	1.59E-32	2.9	7.25E-29	3.09E-33
0.595	1.759	0.856	0.386	1.39E-32	3.0	6.30E-29	3.35E-33
0.584	1.769	0.842	0.381	1.59E-32	2.9	7.14E-29	3.51E-33
0.575	1.778	0.828	0.376	1.51E-32	3.0	6.75E-29	3.64E-33
0.565	1.787	0.813	0.371	1.63E-32	2.9	7.23E-29	3.84E-33
0.556	1.795	0.800	0.366	1.48E-32	3.0	6.53E-29	4.11E-33
0.546	1.804	0.786	0.361	1.52E-32	3.0	6.66E-29	4.42E-33
0.537	1.813	0.773	0.356	1.47E-32	3.0	6.42E-29	4.61E-33
0.528	1.821	0.760	0.351	1.54E-32	3.0	6.68E-29	4.65E-33
0.519	1.829	0.747	0.346	1.64E-32	3.0	7.11E-29	4.56E-33
0.511	1.837	0.735	0.341	1.81E-32	2.9	7.79E-29	4.50E-33
0.502	1.845	0.722	0.336	2.01E-32	2.8	8.63E-29	4.68E-33
0.494	1.852	0.711	0.331	1.90E-32	2.8	8.14E-29	5.10E-33

Table 8b continued:

E' [GeV]	W [GeV]	q^2 [GeV^2]	ε	$\frac{d^2\sigma}{d\Omega dE'}$ $\left[\frac{cm^2}{sterGeV}\right]$	stat. error [%]	$\frac{1}{\Gamma_t}\frac{d^2\sigma}{d\Omega dE'}$ $\left[\frac{cm^2}{ster}\right]$	Rad. correction $\left[\frac{cm^2}{sterGeV}\right]$
0.485	1.859	0.699	0.326	1.70E-32	3.0	7.23E-29	5.59E-33
0.477	1.867	0.687	0.322	1.78E-32	2.9	7.55E-29	5.90E-33
0.469	1.874	0.675	0.317	1.83E-32	2.9	7.75E-29	6.02E-33
0.461	1.881	0.664	0.312	1.90E-32	2.9	8.03E-29	6.15E-33
0.454	1.887	0.653	0.308	2.02E-32	2.8	8.50E-29	6.38E-33
0.446	1.894	0.642	0.303	1.87E-32	2.9	7.83E-29	6.72E-33
0.438	1.901	0.631	0.299	1.90E-32	2.9	7.95E-29	7.03E-33
0.431	1.907	0.620	0.295	2.06E-32	2.8	8.59E-29	7.31E-33
0.424	1.913	0.610	0.290	1.95E-32	2.9	8.12E-29	7.52E-33
0.417	1.920	0.600	0.286	2.02E-32	2.9	8.38E-29	7.66E-33
0.410	1.926	0.590	0.282	2.22E-32	2.8	9.19E-29	7.84E-33
0.403	1.931	0.580	0.278	2.29E-32	2.8	9.46E-29	8.17E-33
0.396	1.937	0.570	0.273	2.10E-32	2.8	8.64E-29	8.72E-33
0.389	1.943	0.561	0.269	2.09E-32	2.9	8.58E-29	9.26E-33
0.383	1.949	0.551	0.265	1.95E-32	2.9	8.02E-29	9.69E-33
0.376	1.954	0.542	0.261	2.08E-32	2.9	8.52E-29	9.92E-33
0.370	1.959	0.533	0.257	2.19E-32	2.8	8.97E-29	1.01E-32
0.364	1.965	0.524	0.253	2.26E-32	2.8	9.25E-29	1.03E-32
0.358	1.970	0.515	0.250	2.25E-32	2.8	9.16E-29	1.06E-32
0.352	1.975	0.506	0.246	2.43E-32	2.8	9.89E-29	1.11E-32
0.346	1.980	0.498	0.242	2.22E-32	2.9	9.02E-29	1.16E-32
0.340	1.985	0.490	0.238	2.27E-32	2.8	9.23E-29	1.20E-32
0.334	1.989	0.481	0.235	2.39E-32	2.8	9.69E-29	1.22E-32
0.329	1.994	0.473	0.231	2.57E-32	2.8	1.04E-28	1.23E-32
0.323	1.999	0.465	0.228	2.39E-32	2.8	9.65E-29	1.32E-32
0.318	2.003	0.458	0.224	2.41E-32	2.8	9.74E-29	1.36E-32

Table 9: Kinematic values and cross sections for the meausrement $E = 1.759$ GeV, $\vartheta = 74.91^\circ$, taken with the three-magnet spectrometer. Cross sections are averaged over two adjacent momentem channels.

E' [GeV]	W [GeV]	q^2 [GeV^2]	ε	$\frac{d^2\sigma}{d\Omega dE'}$ $\left[\frac{cm^2}{sterGeV}\right]$	stat. error [%]	$\frac{1}{\Gamma_t}\frac{d^2\sigma}{d\Omega dE'}$ $\left[\frac{cm^2}{ster}\right]$	Rad. correction $\left[\frac{cm^2}{sterGeV}\right]$
0.679	1.068	1.766	0.339	2.59E-34	19.5	1.52E-29	2.18E-34
0.673	1.080	1.751	0.337	3.37E-36	28.6	1.81E-31	2.21E-34
0.668	1.091	1.737	0.336	1.07E-34	23.6	5.31E-30	2.25E-34
0.662	1.102	1.723	0.334	1.42E-34	23.7	6.53E-30	1.89E-34
0.656	1.115	1.707	0.332	3.38E-34	19.6	1.44E-29	1.50E-34
0.651	1.126	1.693	0.331	6.12E-34	15.9	2.46E-29	1.39E-34
0.645	1.136	1.679	0.329	4.63E-34	17.7	1.76E-29	1.44E-34
0.640	1.147	1.665	0.327	4.11E-34	18.7	1.48E-29	1.42E-34
0.634	1.158	1.650	0.325	6.19E-34	16.3	2.11E-29	1.10E-34
0.629	1.168	1.637	0.324	1.11E-33	12.9	3.62E-29	6.48E-35
0.624	1.177	1.624	0.322	1.23E-33	12.6	3.83E-29	1.61E-35
0.618	1.188	1.608	0.320	1.46E-33	11.9	4.34E-29	-4.39E-35
0.613	1.198	1.596	0.319	2.07E-33	10.1	5.90E-29	-9.22E-35
0.608	1.207	1.583	0.317	2.43E-33	9.4	6.69E-29	-1.34E-34
0.603	1.217	1.569	0.315	2.58E-33	9.2	6.82E-29	-1.42E-34
0.598	1.226	1.555	0.313	2.77E-33	8.8	7.09E-29	-1.24E-34
0.593	1.235	1.543	0.312	2.90E-33	8.6	7.19E-29	-8.86E-35
0.588	1.244	1.530	0.310	2.77E-33	8.8	6.65E-29	-4.25E-35
0.583	1.254	1.516	0.308	2.79E-33	8.7	6.49E-29	1.47E-35
0.578	1.262	1.504	0.307	2.60E-33	9.0	5.88E-29	5.20E-35
0.573	1.270	1.492	0.305	2.90E-33	8.5	6.38E-29	9.37E-35
0.568	1.279	1.479	0.303	2.30E-33	9.4	4.92E-29	1.38E-34
0.563	1.288	1.466	0.301	2.70E-33	8.7	5.63E-29	1.88E-34
0.559	1.295	1.454	0.300	2.19E-33	9.5	4.46E-29	2.37E-34
0.554	1.303	1.442	0.298	2.24E-33	9.4	4.46E-29	2.90E-34
0.549	1.312	1.429	0.296	1.98E-33	9.8	3.84E-29	3.44E-34
0.545	1.320	1.417	0.295	1.80E-33	10.2	3.42E-29	3.67E-34
0.540	1.327	1.406	0.293	1.96E-33	9.9	3.65E-29	3.77E-34
0.536	1.335	1.393	0.291	1.91E-33	10.1	3.49E-29	3.67E-34
0.531	1.343	1.381	0.289	1.97E-33	10.0	3.53E-29	3.49E-34
0.527	1.350	1.370	0.288	2.25E-33	9.5	3.95E-29	3.39E-34
0.522	1.357	1.359	0.286	2.41E-33	9.3	4.16E-29	3.44E-34
0.517	1.365	1.346	0.284	2.05E-33	10.0	3.47E-29	3.53E-34
0.513	1.372	1.336	0.283	2.42E-33	9.3	4.02E-29	3.53E-34
0.509	1.379	1.325	0.281	2.63E-33	9.0	4.31E-29	3.61E-34
0.505	1.386	1.313	0.279	2.50E-33	9.2	4.02E-29	3.90E-34
0.500	1.393	1.302	0.278	2.42E-33	9.3	3.83E-29	4.27E-34
0.496	1.399	1.291	0.276	2.35E-33	9.4	3.67E-29	4.41E-34
0.492	1.406	1.281	0.274	2.63E-33	9.0	4.05E-29	4.28E-34
0.488	1.413	1.269	0.273	3.08E-33	8.5	4.67E-29	4.01E-34
0.484	1.419	1.259	0.271	2.77E-33	9.0	4.13E-29	3.97E-34
0.480	1.425	1.249	0.269	3.43E-33	8.2	5.06E-29	4.24E-34
0.476	1.432	1.238	0.268	2.88E-33	8.8	4.19E-29	4.68E-34
0.472	1.438	1.227	0.266	2.85E-33	8.8	4.09E-29	5.07E-34
0.468	1.444	1.217	0.264	3.16E-33	8.4	4.48E-29	5.38E-34
0.464	1.450	1.207	0.263	3.22E-33	8.4	4.51E-29	5.69E-34
0.460	1.457	1.196	0.261	2.77E-33	8.9	3.83E-29	5.83E-34
0.456	1.462	1.186	0.260	3.40E-33	8.3	4.65E-29	5.41E-34
0.452	1.468	1.177	0.258	3.91E-33	7.9	5.28E-29	4.54E-34
0.448	1.474	1.166	0.256	4.54E-33	7.5	6.07E-29	3.51E-34
0.444	1.480	1.156	0.255	5.00E-33	7.2	6.61E-29	3.22E-34
0.441	1.485	1.147	0.253	4.94E-33	7.2	6.47E-29	4.01E-34
0.437	1.491	1.138	0.252	5.55E-33	6.9	7.19E-29	3.22E-34

Table 10a: Kinematic values and cross sections for the measurement E = 2.835 GeV, $\vartheta = 47.37^\circ$, taken with the three-magnet spectrometer. Cross sections are averaged over two adjacent momentum channels.

E' [GeV]	W [GeV]	q^2 [GeV^2]	ε	$\frac{d^2\sigma}{d\Omega dE'}$ $\left[\frac{cm^2}{sterGeV}\right]$	stat. error [%]	$\frac{1}{\Gamma_t}\frac{d^2\sigma}{d\Omega dE'}$ $\left[\frac{cm^2}{ster}\right]$	Rad. correction $\left[\frac{cm^2}{sterGeV}\right]$
1.371	1.058	2.508	0.584	4.81E-35	21.3	2.21E-30	1.54E-34
1.359	1.079	2.486	0.581	8.07E-35	21.8	3.14E-30	1.14E-34
1.347	1.099	2.465	0.578	2.88E-34	16.0	9.77E-30	7.59E-35
1.336	1.117	2.445	0.575	3.59E-34	14.7	1.09E-29	7.47E-35
1.325	1.135	2.425	0.573	3.11E-34	15.9	8.58E-30	6.34E-35
1.313	1.155	2.402	0.570	4.47E-34	14.2	1.12E-29	2.98E-35
1.303	1.172	2.383	0.567	6.94E-34	12.1	1.61E-29	-3.07E-35
1.292	1.188	2.364	0.564	1.05E-33	10.2	2.26E-29	-1.06E-34
1.281	1.206	2.343	0.561	1.52E-33	8.5	3.06E-29	-1.63E-34
1.270	1.223	2.323	0.558	1.74E-33	7.9	3.29E-29	-1.66E-34
1.259	1.238	2.304	0.556	1.58E-33	8.3	2.83E-29	-1.38E-34
1.249	1.253	2.286	0.553	1.78E-33	7.8	3.03E-29	-1.06E-34
1.237	1.270	2.264	0.550	1.55E-33	8.3	2.50E-29	-7.24E-35
1.228	1.285	2.246	0.547	1.84E-33	7.5	2.85E-29	-4.12E-35
1.218	1.299	2.228	0.544	1.57E-33	8.1	2.34E-29	-5.80E-36
1.207	1.314	2.208	0.542	1.41E-33	8.6	2.01E-29	1.48E-35
1.197	1.329	2.189	0.539	1.61E-33	8.0	2.21E-29	1.40E-35
1.187	1.342	2.172	0.536	1.82E-33	7.6	2.41E-29	1.04E-35
1.177	1.355	2.154	0.533	1.61E-33	8.1	2.07E-29	1.39E-35
1.166	1.370	2.134	0.530	1.67E-33	8.0	2.07E-29	2.77E-35
1.157	1.383	2.117	0.527	1.93E-33	7.4	2.33E-29	3.92E-35
1.148	1.395	2.100	0.524	1.70E-33	7.9	2.00E-29	4.88E-35
1.138	1.409	2.081	0.522	1.83E-33	7.7	2.09E-29	4.62E-35
1.128	1.421	2.063	0.519	2.00E-33	7.4	2.22E-29	3.36E-35
1.119	1.433	2.047	0.516	2.15E-33	7.2	2.33E-29	2.57E-35
1.110	1.445	2.030	0.513	2.20E-33	7.1	2.33E-29	3.26E-35
1.099	1.458	2.011	0.510	2.42E-33	6.8	2.51E-29	2.83E-35
1.090	1.469	1.995	0.507	2.36E-33	7.0	2.40E-29	-2.81E-35
1.082	1.480	1.979	0.504	3.14E-33	6.2	3.13E-29	-1.35E-34
1.072	1.492	1.962	0.501	3.87E-33	5.7	3.78E-29	-2.58E-34
1.063	1.504	1.945	0.498	4.35E-33	5.4	4.16E-29	-3.13E-34
1.054	1.514	1.929	0.496	4.58E-33	5.3	4.30E-29	-2.77E-34
1.046	1.525	1.913	0.493	4.45E-33	5.3	4.11E-29	-1.86E-34
1.036	1.536	1.895	0.490	4.30E-33	5.3	3.91E-29	-6.35E-35
1.028	1.546	1.880	0.487	4.13E-33	5.4	3.69E-29	1.50E-35
1.019	1.556	1.865	0.484	3.97E-33	5.5	3.50E-29	8.66E-35
1.010	1.567	1.849	0.481	3.97E-33	5.5	3.44E-29	1.62E-34
1.002	1.577	1.833	0.478	3.56E-33	5.7	3.04E-29	2.31E-34
0.994	1.587	1.818	0.476	3.47E-33	5.8	2.92E-29	2.87E-34
0.985	1.596	1.803	0.473	3.49E-33	5.8	2.90E-29	3.29E-34
0.976	1.607	1.786	0.470	3.27E-33	6.0	2.68E-29	3.42E-34
0.968	1.616	1.772	0.467	3.43E-33	5.9	2.78E-29	3.06E-34
0.961	1.625	1.758	0.464	3.92E-33	5.6	3.14E-29	2.50E-34
0.952	1.634	1.742	0.461	4.18E-33	5.5	3.31E-29	1.92E-34
0.944	1.644	1.727	0.458	4.55E-33	5.3	3.56E-29	1.50E-34
0.936	1.652	1.713	0.456	4.71E-33	5.3	3.65E-29	1.29E-34
0.929	1.661	1.699	0.453	5.30E-33	5.0	4.07E-29	1.20E-34
0.920	1.670	1.683	0.450	5.11E-33	5.1	3.88E-29	1.13E-34
0.913	1.678	1.670	0.447	6.01E-33	4.7	4.52E-29	8.48E-35
0.905	1.687	1.657	0.445	5.72E-33	4.9	4.26E-29	3.97E-35
0.897	1.695	1.642	0.442	6.70E-33	4.6	4.94E-29	1.15E-35

Table 10b: Kinematic values and cross sections for the measurement $E = 2.835$ GeV, $\vartheta = 47.37^{\circ}$, taken with the three-magnet spectrometer. Cross sections are averaged over four adjacent momentum channels.

E' [GeV]	W [GeV]	q^2 [GeV^2]	ε	$\frac{d^2\sigma}{d\Omega dE'}$ $\left[\frac{cm^2}{sterGeV}\right]$	stat. error [%]	$\frac{1}{\Gamma_t}\frac{d^2\sigma}{d\Omega dE'}$ $\left[\frac{cm^2}{ster}\right]$	Rad. correction $\left[\frac{cm^2}{sterGeV}\right]$
1.376	1.048	2.518	0.585	5.35E-35	14.1	2.68E-30	1.76E-34
1.353	1.089	2.476	0.579	1.30E-34	12.9	4.72E-30	1.49E-34
1.331	1.126	2.435	0.574	3.68E-34	10.8	1.07E-29	3.53E-35
1.308	1.163	2.393	0.568	6.32E-34	9.2	1.52E-29	-6.24E-35
1.286	1.197	2.354	0.563	1.26E-33	6.5	2.64E-29	-1.16E-34
1.264	1.230	2.314	0.557	1.63E-33	5.7	3.01E-29	-1.27E-34
1.243	1.262	2.275	0.551	1.66E-33	5.7	2.75E-29	-8.53E-35
1.223	1.292	2.237	0.546	1.71E-33	5.5	2.59E-29	-2.70E-35
1.202	1.321	2.199	0.540	1.51E-33	5.9	2.11E-29	1.77E-35
1.182	1.349	2.163	0.535	1.69E-33	5.5	2.21E-29	3.62E-35
1.162	1.377	2.125	0.529	1.78E-33	5.4	2.18E-29	5.22E-35
1.143	1.402	2.090	0.523	1.75E-33	5.5	2.03E-29	6.02E-35
1.123	1.427	2.055	0.517	2.06E-33	5.2	2.26E-29	4.57E-35
1.104	1.452	2.021	0.511	2.36E-33	4.9	2.48E-29	-2.42E-35
1.086	1.475	1.987	0.506	2.80E-33	4.7	2.82E-29	-1.30E-34
1.067	1.498	1.953	0.500	4.03E-33	3.9	3.89E-29	-2.05E-34
1.050	1.519	1.921	0.494	4.45E-33	3.7	4.15E-29	-1.70E-34
1.032	1.541	1.888	0.488	4.21E-33	3.8	3.79E-29	-2.13E-35
1.015	1.562	1.857	0.483	3.95E-33	3.9	3.45E-29	1.48E-34
0.998	1.582	1.825	0.477	3.49E-33	4.1	2.96E-29	2.84E-34
0.981	1.601	1.795	0.471	3.40E-33	4.2	2.81E-29	3.19E-34
0.965	1.620	1.765	0.466	3.68E-33	4.1	2.96E-29	2.76E-34
0.948	1.639	1.735	0.460	4.34E-33	3.8	3.42E-29	1.93E-34
0.933	1.656	1.706	0.454	5.02E-33	3.6	3.87E-29	1.18E-34
0.916	1.674	1.677	0.449	5.58E-33	3.5	4.21E-29	8.39E-35
0.901	1.691	1.649	0.443	6.12E-33	3.3	4.54E-29	1.16E-34
0.886	1.708	1.621	0.437	6.74E-33	3.2	4.90E-29	2.13E-34
0.871	1.724	1.594	0.432	5.81E-33	3.4	4.16E-29	3.29E-34
0.857	1.739	1.568	0.426	6.69E-33	3.2	4.71E-29	4.44E-34
0.842	1.755	1.541	0.421	6.23E-33	3.3	4.32E-29	5.57E-34
0.828	1.769	1.516	0.415	6.24E-33	3.3	4.27E-29	6.57E-34
0.814	1.784	1.489	0.410	6.27E-33	3.3	4.23E-29	7.67E-34
0.801	1.798	1.465	0.405	5.87E-33	3.4	3.91E-29	8.52E-34
0.787	1.812	1.440	0.399	6.62E-33	3.2	4.36E-29	9.42E-34
0.774	1.825	1.416	0.394	6.00E-33	3.4	3.90E-29	9.86E-34
0.761	1.838	1.392	0.389	6.47E-33	3.3	4.17E-29	9.76E-34
0.748	1.851	1.369	0.383	7.32E-33	3.2	4.67E-29	9.47E-34
0.736	1.864	1.346	0.378	8.01E-33	3.1	5.06E-29	9.80E-34
0.723	1.876	1.323	0.373	7.86E-33	3.1	4.92E-29	1.12E-33
0.711	1.888	1.301	0.368	7.95E-33	3.1	4.93E-29	1.27E-33
0.699	1.900	1.279	0.363	7.38E-33	3.2	4.54E-29	1.39E-33
0.687	1.911	1.258	0.358	8.25E-33	3.1	5.03E-29	1.41E-33
0.676	1.922	1.237	0.353	8.84E-33	3.0	5.35E-29	1.41E-33

Table 11: Cross sections from coincidence measurements for π^0-Electroproduction ($\phi = 0^\circ$)

W [MeV]	$\Theta_{p,CM}$ [o]	q^2 [f^{-2}]	$\frac{d^3\sigma}{d\Omega dE' d\Omega_{p,CM}}$ [$10^{-33}\frac{cm^2}{ster^2 GeV}$]
E = 1,408 GeV; $\vartheta_e = 55^\circ$			
1086	88	23,2	0,10 ± 50%
1116	30	22,7	0,18 ± 24%
1114	60	22,7	0,38 ± 19%
1117	86	22,6	0,51 ± 16%
1117	113	22,6	0,32 ± 27%
1117	167	22,6	0,19 ± 30%
1176	85	21,0	1,60 ± 22%
1233	27	19,8	1,09 ± 12%
1245	88	19,7	2,13 ± 10%
1230	167	20,0	1,13 ± 25%
1307	90	18,1	1,26 ± 37%
1380	90	16,1	1,10 ± 28%
E = 1,198 GeV; $\vartheta_e = 75^\circ$			
1150	88	22,5	0,37 ± 20%
1236	89	20,0	1,09 ± 16%
1369	89	15,6	0,36 ± 50%

Figure captions:

Figure 1: $\frac{d^2\sigma}{d\Omega dE'}$ versus secondary energy E' of the electron for E = 1.531 GeV, $\vartheta = 47.4^\circ$ ($q^2_{1236} = 19.7\ f^{-2}$).

Figure 2: $\frac{1}{\Gamma_t}\frac{d^2\sigma}{d\Omega dE'}$ versus secondary energy E' of the electron for E = 2.231 GeV, $\vartheta = 47.4^\circ$ ($q^2_{1236} = 39.5\ f^{-2}$).

Figure 3: dto. for E = 2.835 GeV, $\vartheta = 47.4^\circ$ ($q^2_{1236} = 59.2\ f^{-2}$).

Figure 4: dto. for E = 2.913 GeV, $\vartheta = 32.2^\circ$ ($q^2_{1236} = 40.0\ f^{-2}$).

Figure 5: "Rosenbluth" plot for $q^2 = 20\ f^{-2}$, W = 1236 MeV. The straight lines are theoretical predictions[14].

Figure 6: dto. for $q^2 = 40\ f^{-2}$, W = 1236 MeV.

Figure 7: dto. for $q^2 = 17\ f^{-2}$, W = 1350 MeV.

Figure 8: dto. for $q^2 = 35\ f^{-2}$, W = 1350 MeV.

Figure 9: $\frac{1}{\Gamma_t}\frac{d^2\sigma}{d\Omega dE'} \cdot \left(\frac{G_{MP}(o)}{G_{MP}(q^2)}\right)^2$ versus $|\vec{q}|^2$ for W = 1236 MeV. Curve α) dispersion theoretic model[14], curve β) dispersion theoretic model[15], and curve γ) $\mathfrak{d}(12)$ prediction[13].

Figure 10-13: $\frac{1}{\Gamma_t}\frac{d^2\sigma}{d\Omega dE'} \cdot \left(\frac{G_{MP}(o)}{G_{MP}(q^2)}\right)^2$ versus $|\vec{q}|^2$ for the masses W = 1420, 1525, 1615, 1688 and 1820 MeV. For 1525 and 1688 also the resonant part alone is shown.

Figure 14: Exponent b from $\frac{1}{\Gamma_t}\frac{d^2\sigma}{d\Omega dE'} \cdot \left(\frac{G_{MP}(o)}{G_{MP}(q^2)}\right)^2 \approx |\vec{q}|^b$ versus W.

Figure 15: Coincidence cross sections for π^o-production versus W at E = 1.408 GeV, $\Theta_{p,CM} \approx 90^\circ$ and a) $\vartheta = 55^\circ$, b) $\vartheta = 75^\circ$. The curves are the dispersion theoretic model[14].

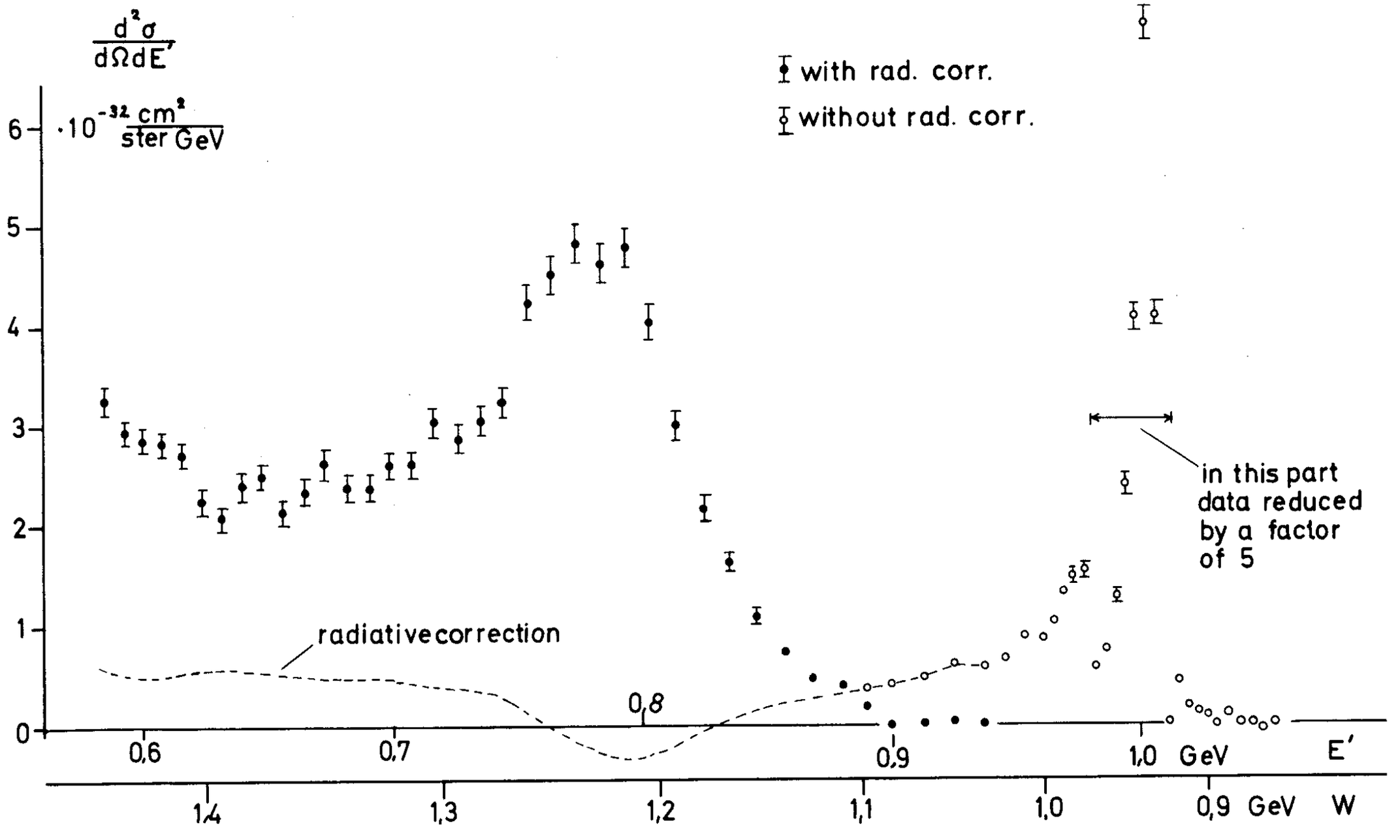
$\frac{d^2\sigma}{d\Omega dE'}$
$\cdot 10^{-32} \frac{cm^2}{ster\ GeV}$
with rad. corr.
without rad. corr.
in this part data reduced by a factor of 5
radiative correction
0,8
0,6
0,7
0,9
1,0 GeV
E'
1,4
1,3
1,2
1,1
1,0
0,9 GeV
W

Fig. 1

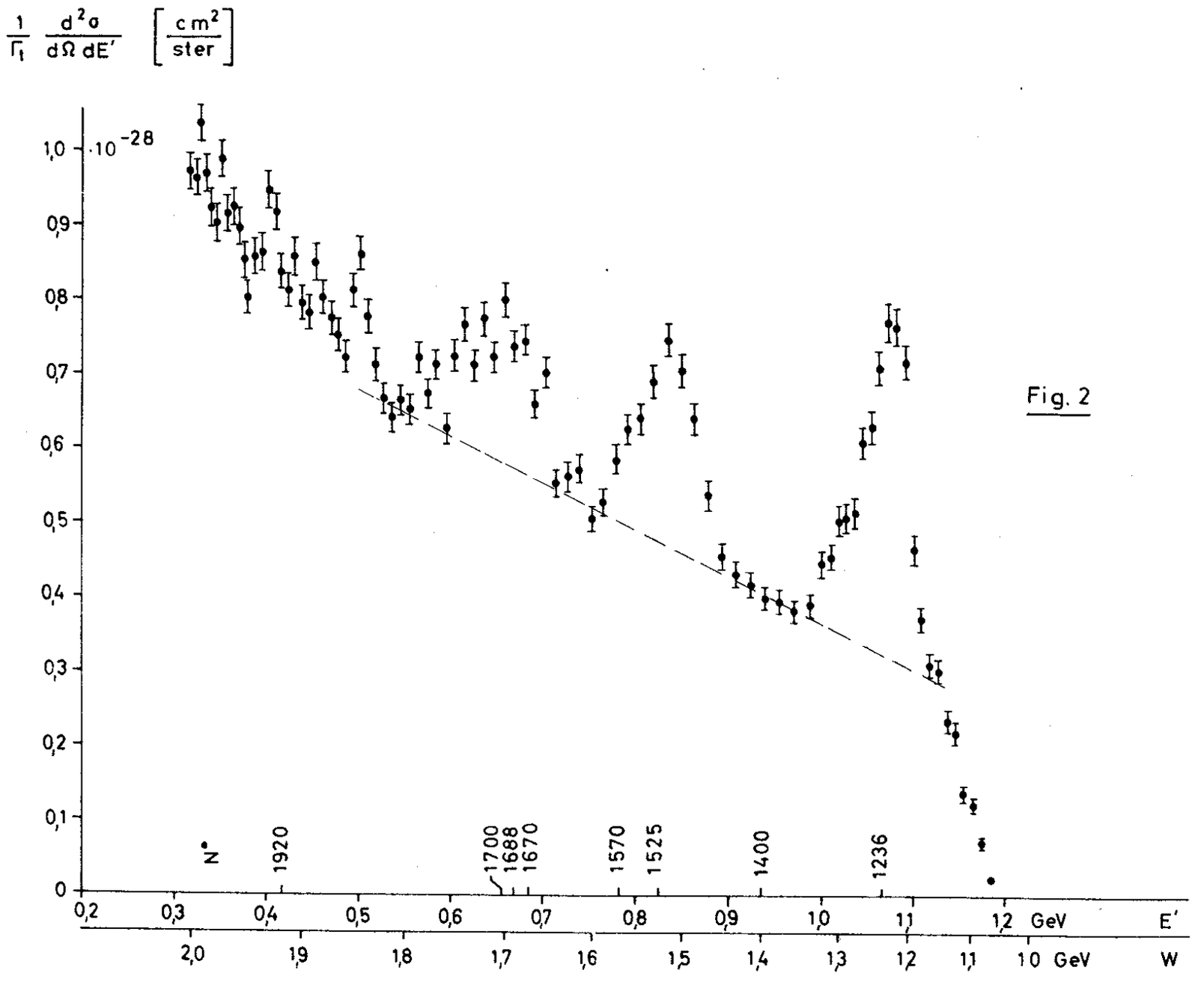
$\frac{1}{\Gamma_t}\frac{d^2\sigma}{d\Omega\, dE'}$ $\left[\frac{cm^2}{ster}\right]$
$\cdot 10^{-28}$
1,0
0,9
0,8
0,7
0,6
0,5
0,4
0,3
0,2
0,1
0
N*
1920
1700
1688
1670
1570
1525
1400
1236
0,2
0,3
0,4
0,5
0,6
0,7
0,8
0,9
1,0
1,1
1,2 GeV
E'
2,0
1,9
1,8
1,7
1,6
1,5
1,4
1,3
1,2
1,1
1,0 GeV
W

Fig. 2

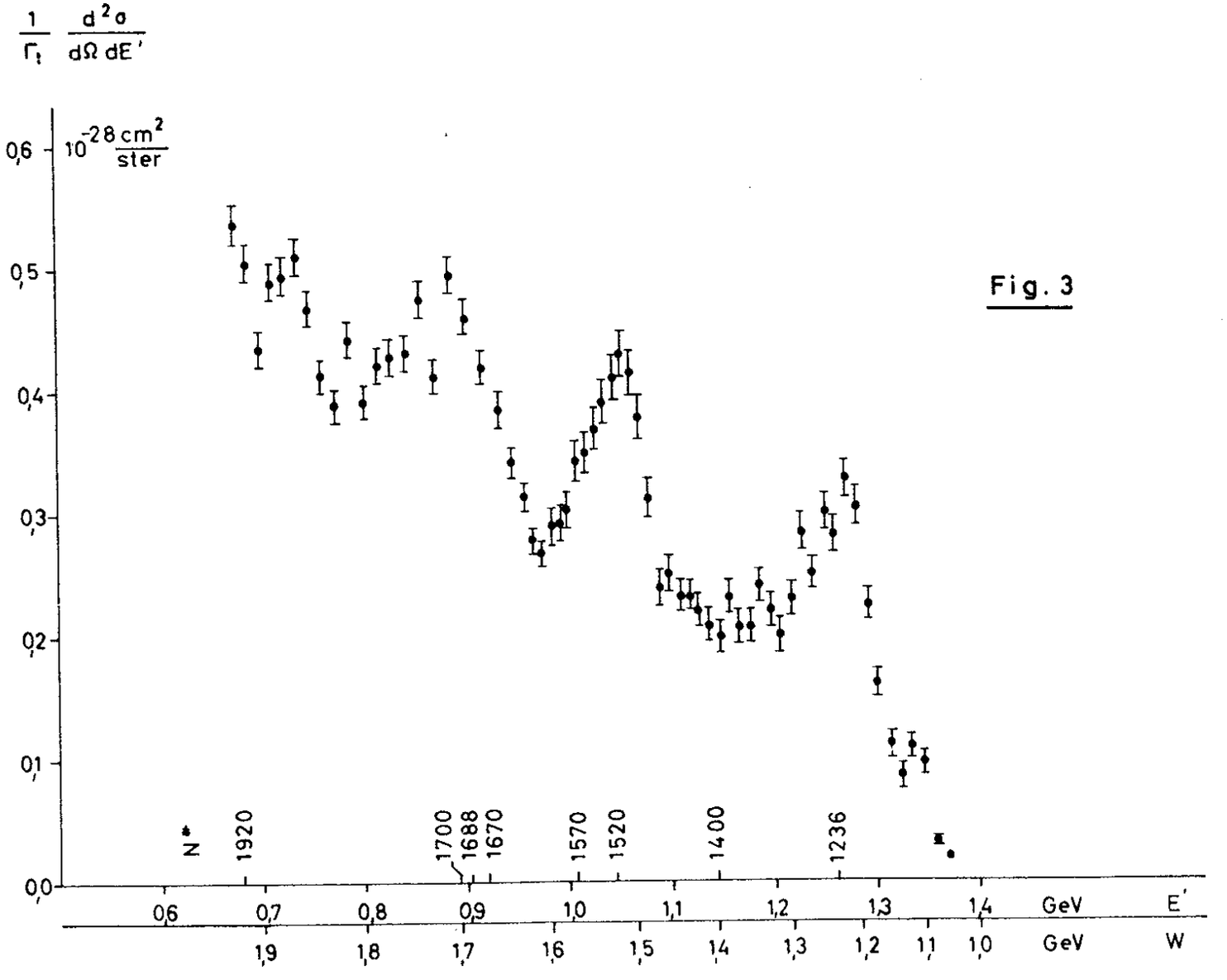
1/Γt dσ²/dΩ dE'
10⁻²⁸ cm²/ster
0,6
0,5
0,4
0,3
0,2
0,1
0,0
N*
1920
1700
1688
1670
1570
1520
1400
1236
0,6
0,7
0,8
0,9
1,0
1,1
1,2
1,3
1,4
GeV
E'
1,9
1,8
1,7
1,6
1,5
1,4
1,3
1,2
1,1
1,0
GeV
W

Fig. 3

$\frac{1}{\Gamma_t} \cdot \frac{d^2\sigma}{d\Omega\, dE'}$

Fig. 4

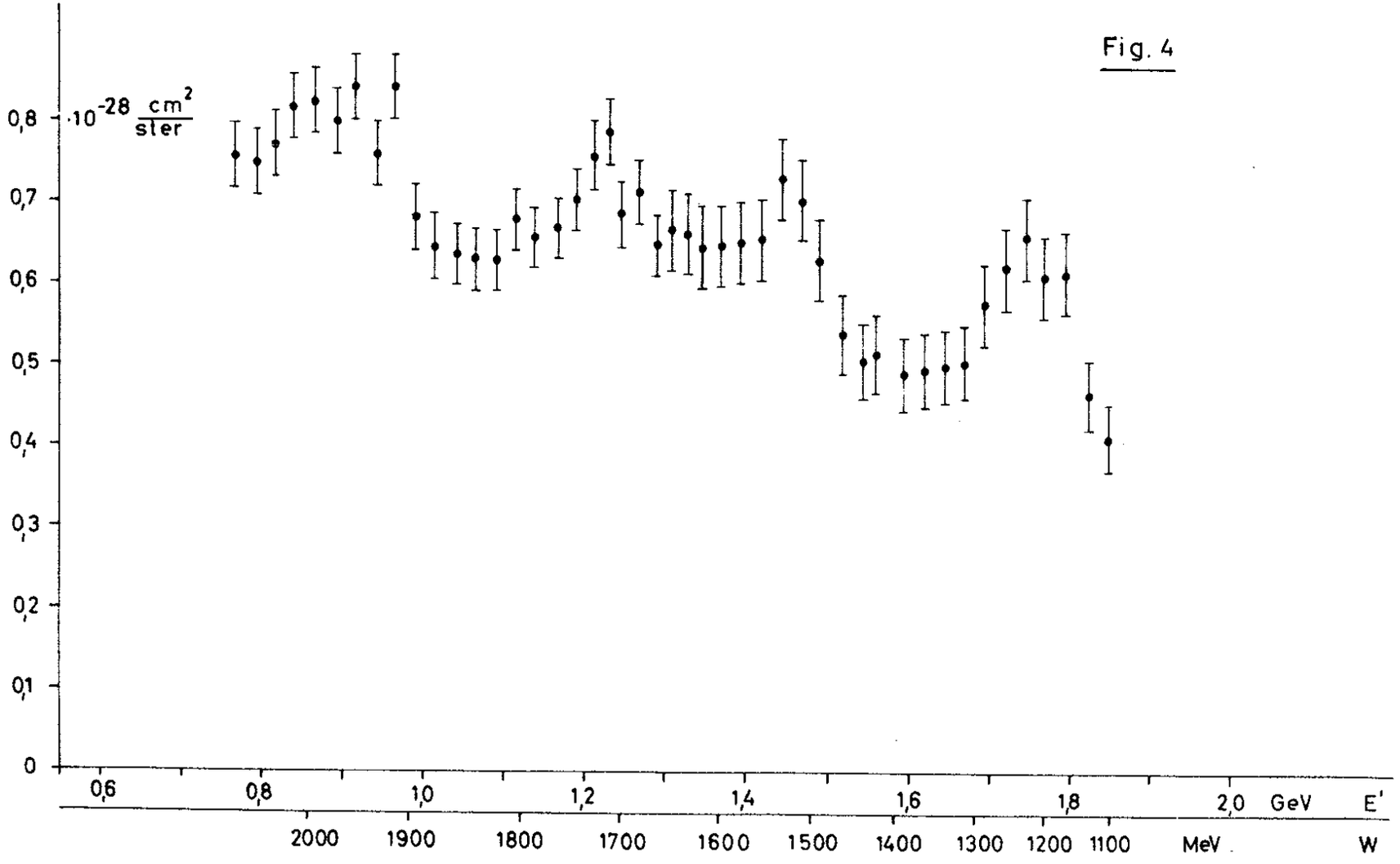

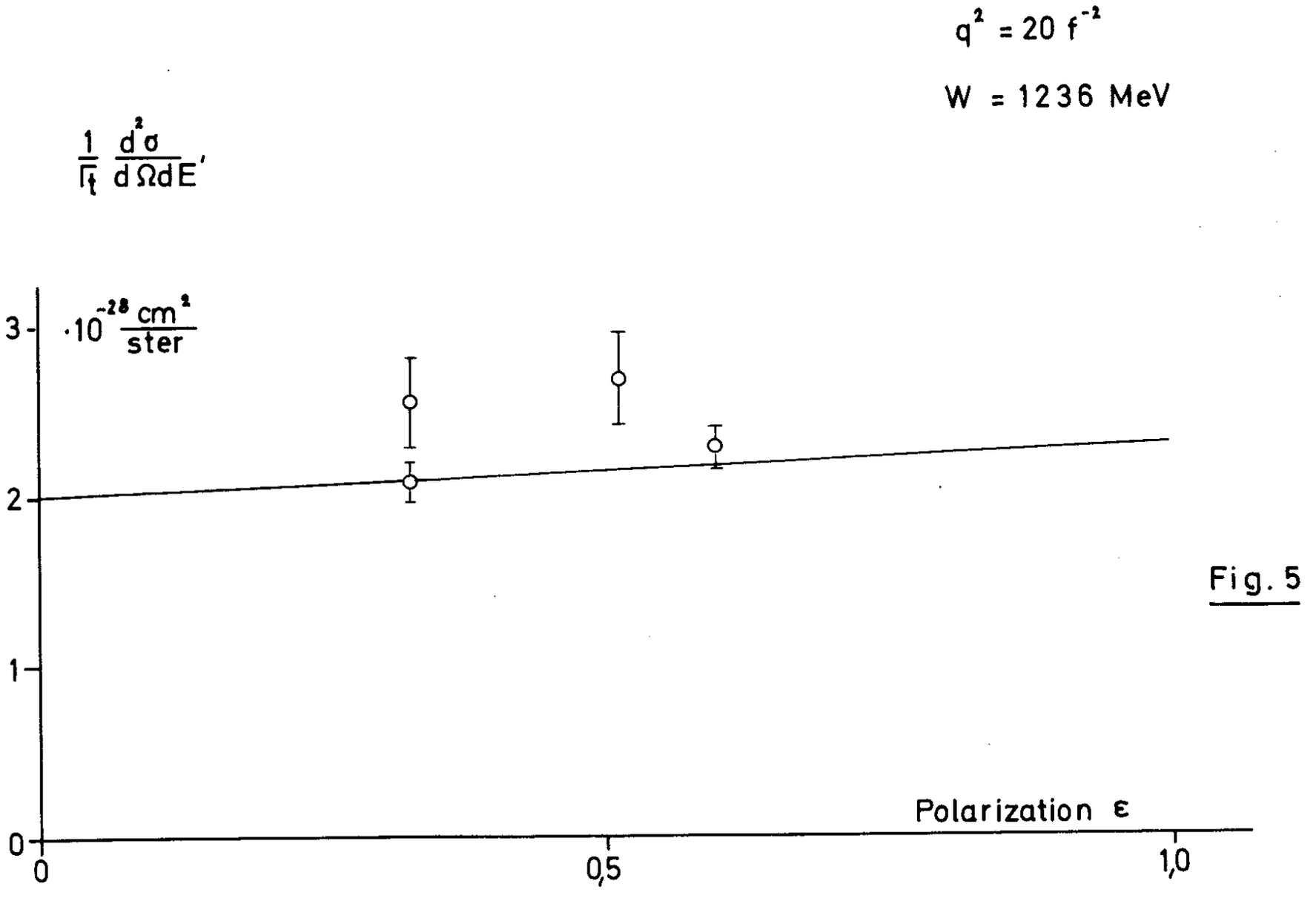
$q^2 = 20\ f^{-2}$
W = 1236 MeV
$\frac{1}{\Gamma_t}\frac{d^2\sigma}{d\Omega dE'}$
$\cdot 10^{-28}\frac{cm^2}{ster}$
3
2
1
0
0
0,5
1,0
Polarization ε

Fig. 5

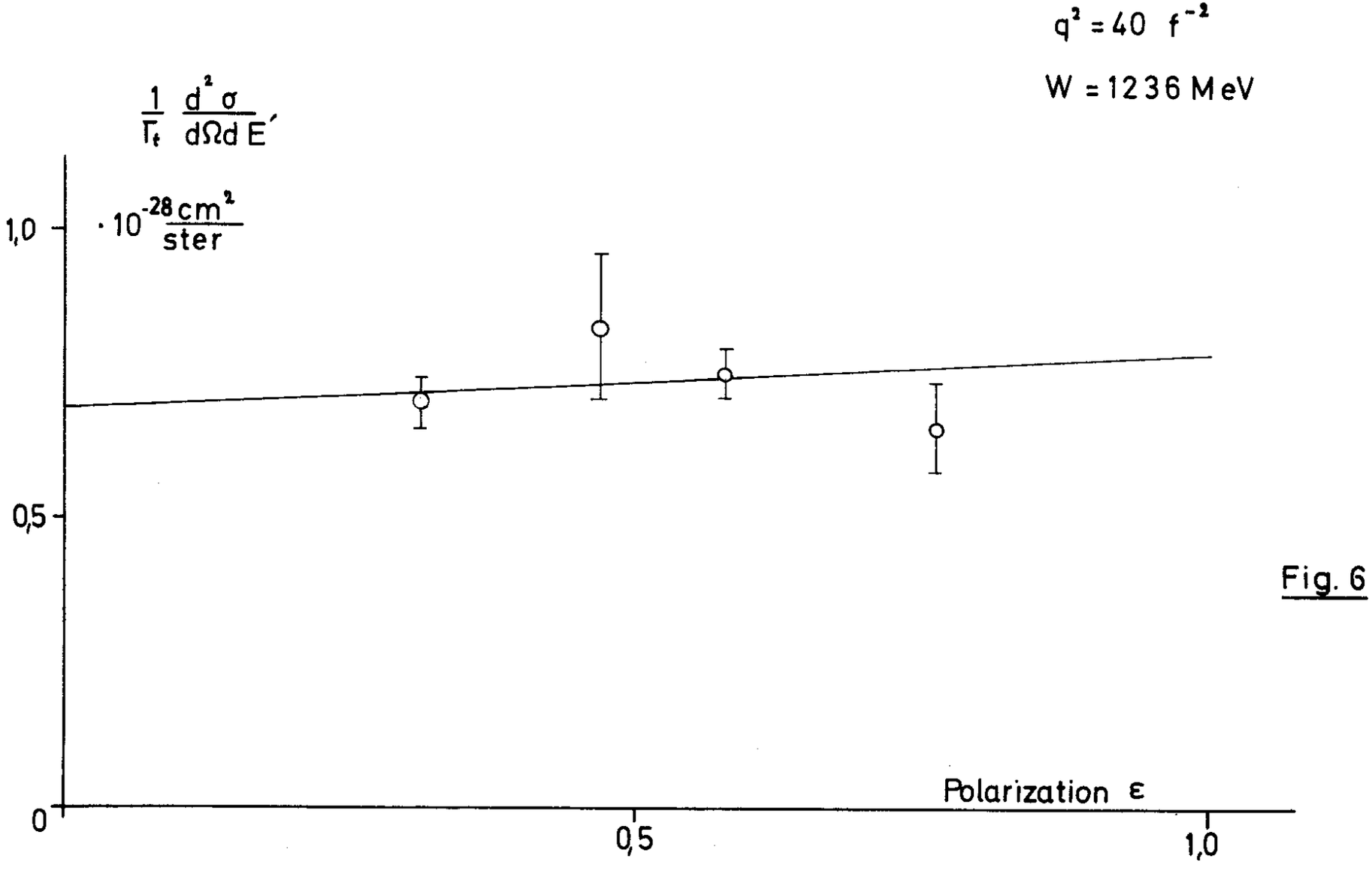
$q^2 = 40\ f^{-2}$
W = 1236 MeV
$\frac{1}{\Gamma_t}\frac{d^2\sigma}{d\Omega d E'}$
$\cdot 10^{-28}\frac{cm^2}{ster}$
1,0
0,5
0
0,5
1,0
Polarization ε

Fig. 6

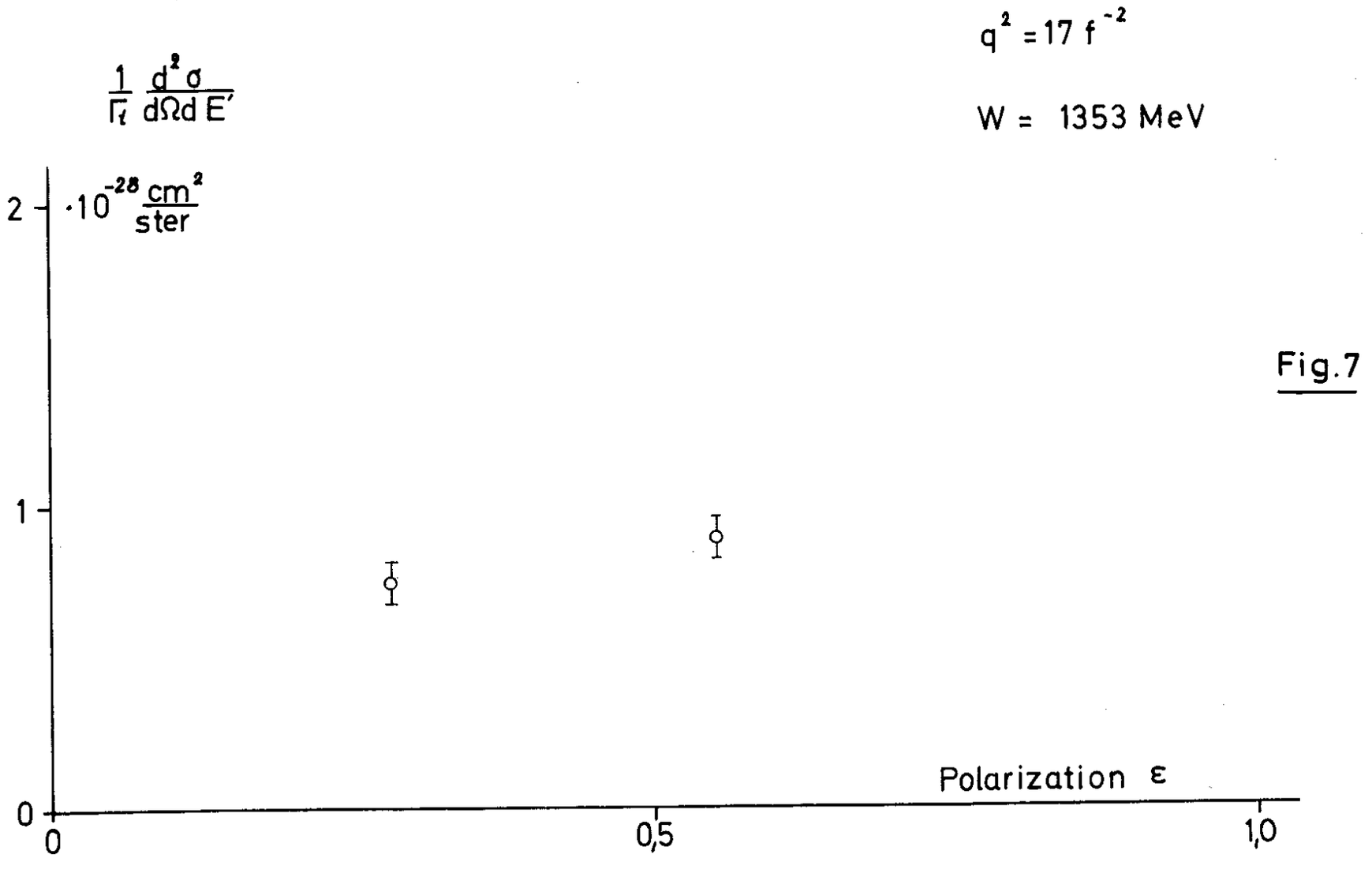
$q^2 = 17\ f^{-2}$
W = 1353 MeV
$\frac{1}{\Gamma_t}\frac{d^2\sigma}{d\Omega d E'}$
$\cdot 10^{-28}\frac{cm^2}{ster}$
2
1
0
0
0,5
1,0
Polarization ε

Fig.7

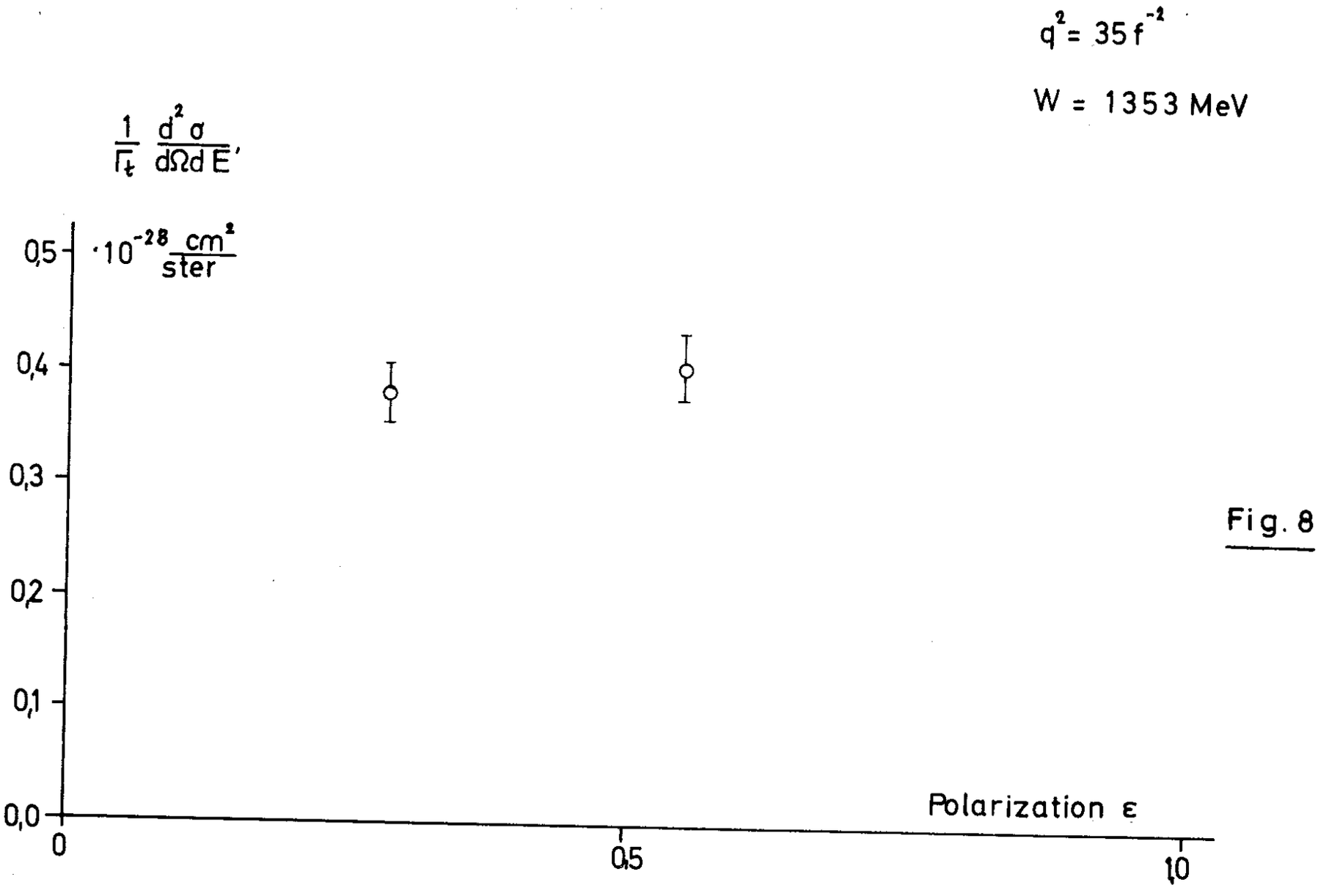
$q^2 = 35\,f^{-2}$
W = 1353 MeV
$\frac{1}{\Gamma_t}\frac{d^2\sigma}{d\Omega dE'}$
$\cdot 10^{-28}\frac{cm^2}{ster}$
0,5
0,4
0,3
0,2
0,1
0,0
0
0,5
1,0
Polarization ε

Fig. 8

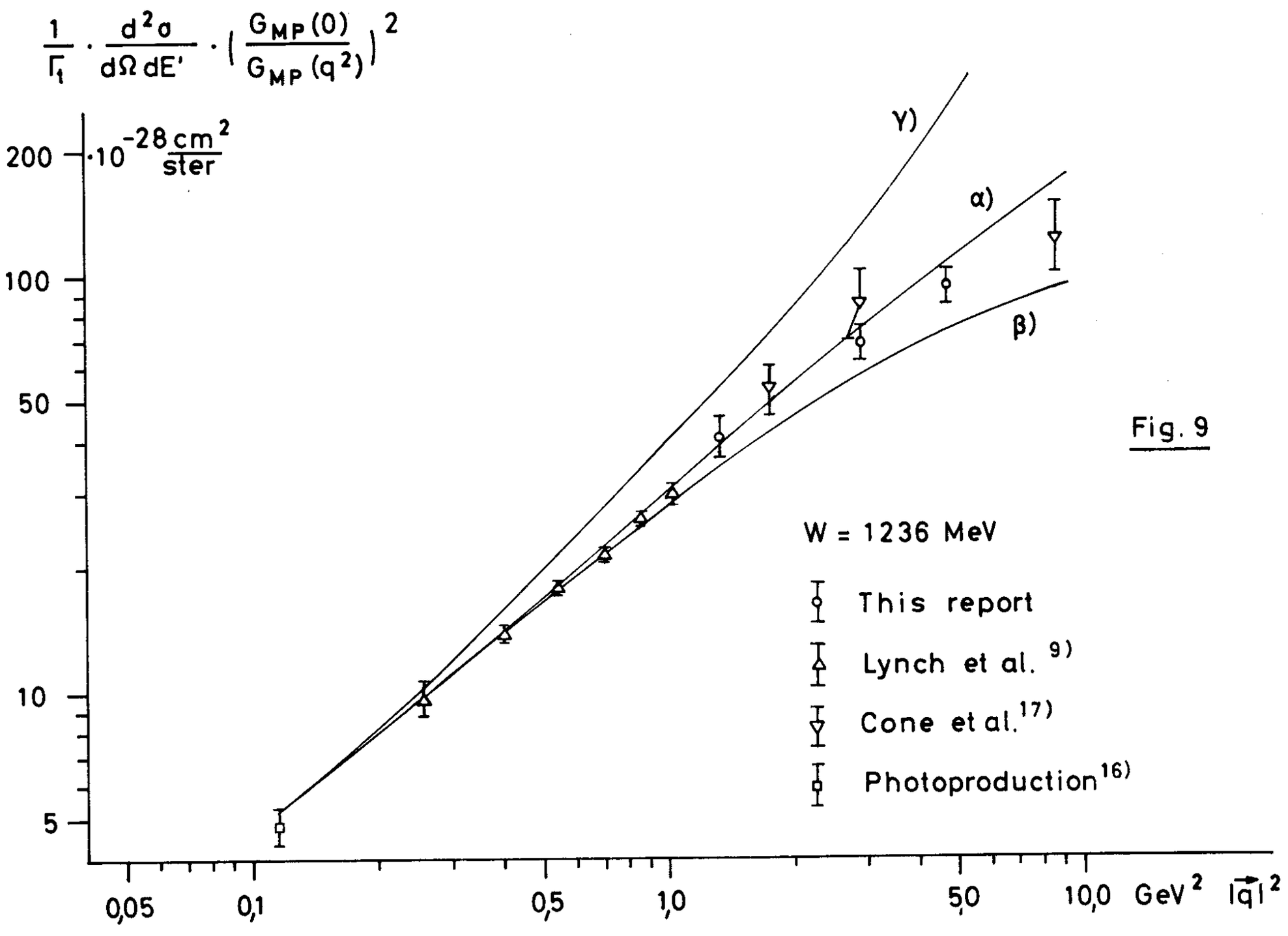
$\frac{1}{\Gamma_t} \cdot \frac{d^2\sigma}{d\Omega\, dE'} \cdot \left(\frac{G_{MP}(0)}{G_{MP}(q^2)}\right)^2$
$\cdot 10^{-28} \frac{cm^2}{ster}$
200
100
50
10
5
γ)
α)
β)
W = 1236 MeV
This report
Lynch et al. 9)
Cone et al. 17)
Photoproduction 16)
0,05
0,1
0,5
1,0
5,0
10,0 GeV^2 $|\vec{q}|^2$

Fig. 9

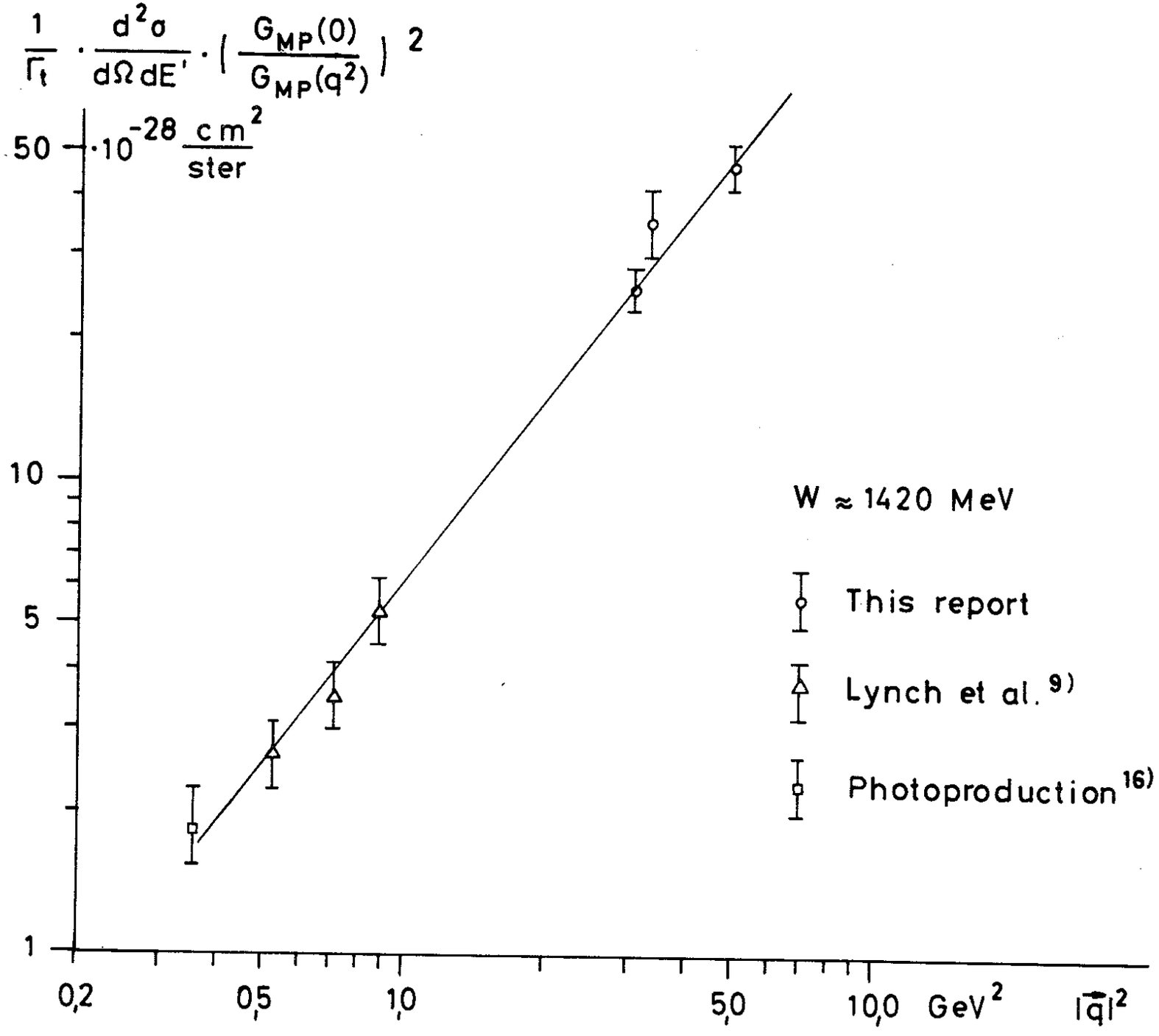
$\frac{1}{\Gamma_t} \cdot \frac{d^2\sigma}{d\Omega\, dE'} \cdot \left(\frac{G_{MP}(0)}{G_{MP}(q^2)} \right)^2$
$\cdot 10^{-28} \frac{cm^2}{ster}$
50
10
5
1
0,2
0,5
1,0
5,0
10,0 GeV^2
$|\vec{q}|^2$
W ≈ 1420 MeV
This report
Lynch et al. 9)
Photoproduction 16)

Fig.10

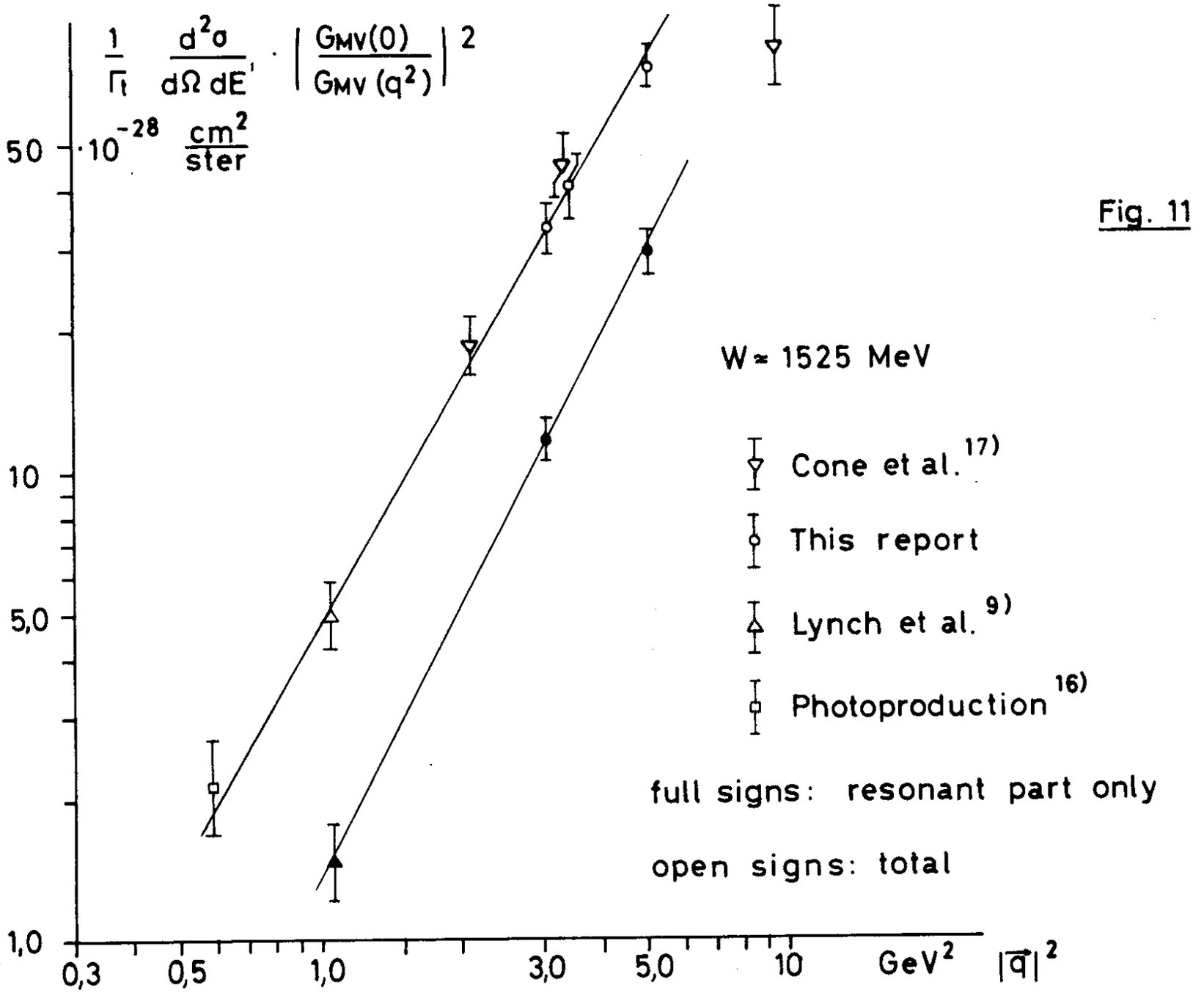
$\frac{1}{\Gamma_t} \frac{d^2\sigma}{d\Omega\, dE'} \cdot \left| \frac{G_{MV}(0)}{G_{MV}(q^2)} \right|^2$
$\cdot 10^{-28} \frac{cm^2}{ster}$
50
10
5,0
1,0
0,3
0,5
1,0
3,0
5,0
10
GeV^2
$|\vec{q}|^2$
W = 1525 MeV
Cone et al. [17]
This report
Lynch et al. [9]
Photoproduction [16]
full signs: resonant part only
open signs: total

Fig. 11

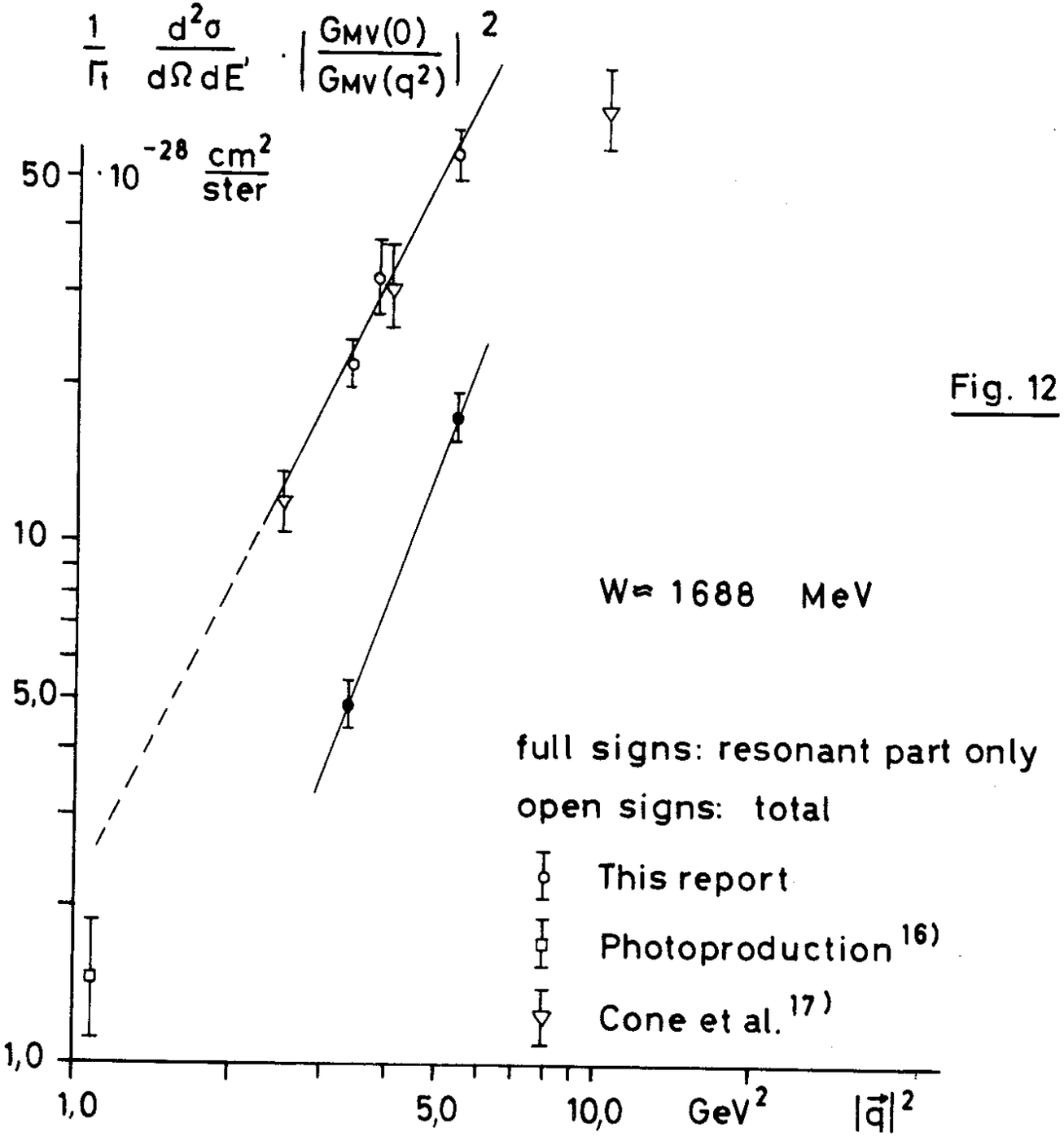
$\frac{1}{\Gamma_t}\ \frac{d^2\sigma}{d\Omega\, dE'} \cdot \left|\frac{G_{MV}(0)}{G_{MV}(q^2)}\right|^2$
$\cdot 10^{-28}\ \frac{cm^2}{ster}$
50
10
5,0
1,0
1,0
5,0
10,0
GeV^2
$|\vec{q}|^2$
W= 1688 MeV
full signs: resonant part only
open signs: total
This report
Photoproduction [16)]
Cone et al. [17)]

Fig. 12

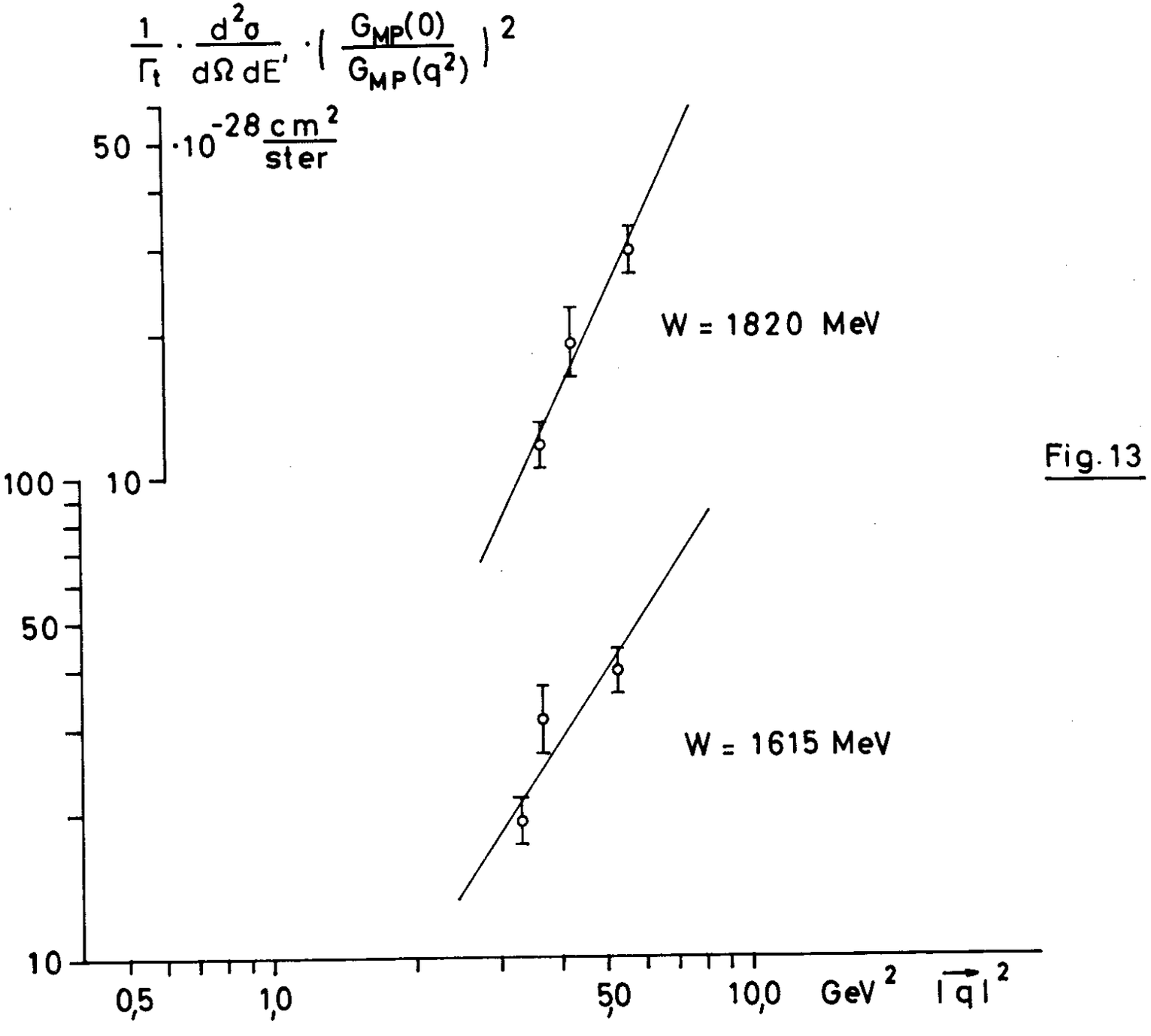
$\frac{1}{\Gamma_t} \cdot \frac{d^2\sigma}{d\Omega\, dE'} \cdot \left(\frac{G_{MP}(0)}{G_{MP}(q^2)} \right)^2$
50
$\cdot 10^{-28} \frac{cm^2}{ster}$
10
100
50
10
W = 1820 MeV
W = 1615 MeV
0,5
1,0
5,0
10,0
GeV^2
$|\vec{q}|^2$

Fig. 13

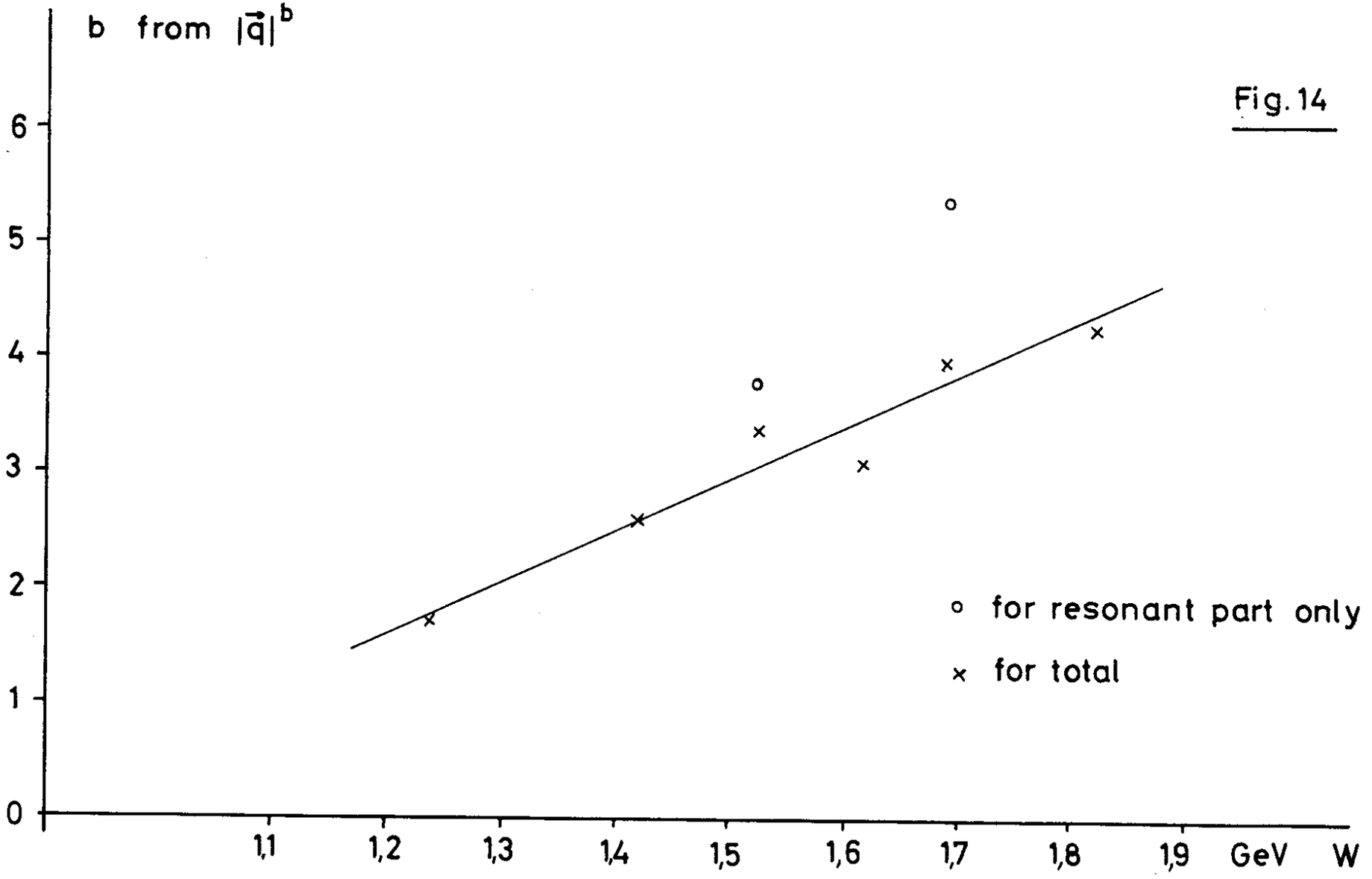
b from $|\vec{q}|^b$
6
5
4
3
2
1
0
1,1
1,2
1,3
1,4
1,5
1,6
1,7
1,8
1,9
GeV
W
o for resonant part only
× for total

Fig. 14

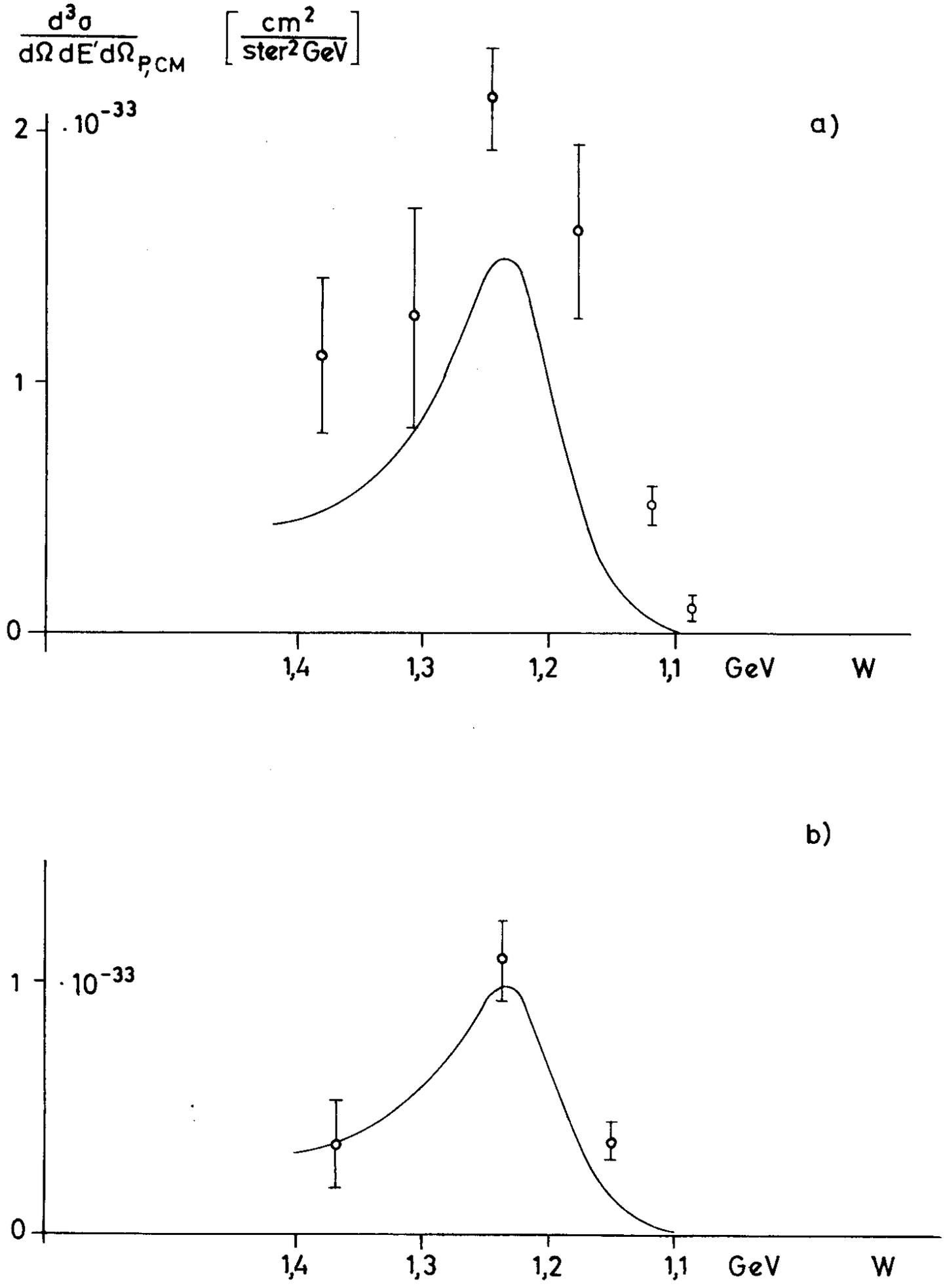
$\frac{d^3\sigma}{d\Omega\, dE' d\Omega_{P,CM}}$ $\left[\frac{cm^2}{ster^2\, GeV}\right]$
a)
2
$\cdot 10^{-33}$
1
0
1,4
1,3
1,2
1,1
GeV
W
b)
1
$\cdot 10^{-33}$
0
1,4
1,3
1,2
1,1
GeV
W

Fig.15